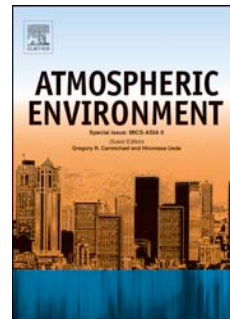# Accepted Manuscript

Identification of fine (PM$_1$) and coarse (PM$_{10\text{-}1}$) sources of particulate matter in an urban environment

G. Titos, H. Lyamani, M. Pandolfi, A. Alastuey, L. Alados-Arboledas

1   **Identification of fine (PM$_1$) and coarse (PM$_{10\text{-}1}$) sources of particulate matter in an**

2   **urban environment**

3

4   **Titos G.[1,2], Lyamani H.[1,2], Pandolfi, M.[3], Alastuey A.[3], and Alados-Arboledas L.[1,2]**

5

6   [1]Department of Applied Physics, Sciences Faculty, University of Granada, 18071, Granada,

7   Spain.

8   [2]Andalusian Institute for Earth System Research, IISTA-CEAMA, University of Granada,

9   Junta de Andalucía, Granada, 18006, Spain

10   [3]Institute of Environmental Assessment and Water Research (IDÆA), Department of

11   Geosciences, CSIC, Barcelona, Spain.

12

13

14   Correspondence to: Gloria Titos Vela. Departamento de Física Aplicada, Universidad de

15   Granada, Granada, Spain.

16   **Phone:** +34 958249754

17   **E-mail**: gtitos@ugr.es

18

19

20 **Abstract**

21 PM_{10} and PM_1 samples were collected at an urban site in southeastern Spain during 2006-

22 2010. The chemical composition of all samples has been determined and analyzed by

23 Positive Matrix Factorization (PMF) technique for fine and coarse source identification.

24 The PMF results have been analyzed for working and non-working days in order to

25 evaluate the change in PM sources contribution and possible future abatement strategies. A

26 decreasing trend in PM_{10} levels and in its constituents has been observed, being partly

27 associated to a reduction in anthropogenic activities due to the economic crisis. The use of

28 fine and coarse PM in the PMF analysis allowed us for the identification of additional

29 sources that could not be identified using only one size fraction. The mineral dust source

30 was identified in both fractions and comprised 36 and 22% of the total mass in the coarse

31 and fine fractions, respectively. This high contribution of the mineral source to the fine

32 fraction may be ascribed to contamination of the source profile. The regional re-circulation

33 source was traced by secondary sulfate, V and Ni. It was the most important source

34 concerning PM_1 mass concentration (41% of the total mass in this fraction). Although V

35 and Ni are commonly associated to fuel oil combustion the seasonality of this source with

36 higher concentrations in summer compared with winter suggest that the most important part

37 of this source can be ascribed to regional pollution episodes. A traffic exhaust source was

38 identified but only in the fine fraction, comprising 29% of the fine mass. The celestite

39 mines source associated with nearby open-pit mines was typified by strontium, sulfate and

40 mineral matter. PM_{10-1} levels were higher in working days, whereas PM_1 levels remained

41 fairly constant throughout the whole week. As a conclusion, traffic seems to be the main

42 source to target in Granada.

43   **Keywords:** PMF, source apportionment, PM1, PM10, urban aerosols

44   **1. Introduction**

45   Particulate matter (PM) is a pollutant of great concern nowadays due to its negative effects

46   on human health (Pope and Dockery, 2006). Apart of its harmful effects on human heath,

47   PM also affects visibility and alters the Earth's radiative balance (Forster et al., 2007). For

48   these reasons, European directive 2008/50/EC regulates the levels of PM_{10} (particles with

49   an aerodynamic diameter <10 μm) setting the daily limit in 50 μg/m^3 that cannot be exceed

50   more than 35 times per year and the annual limit in 40 μg/m^3. In addition to PM_{10}, $PM_{2.5}$

51   (particles with an aerodynamic diameter <2.5 μm) is also regulated in the European

52   directives (annual limit value of 25 µg/m^3 mandatory for 2015), however, there is no

53   regulation concerning PM_1 (particles with an aerodynamic diameter <1 μm). This fact

54   evidences a gap in the European legislation because it is well known that most

55   anthropogenic pollutants tend to accumulate in the finer fractions and that fine particles

56   present harmful effects on human health (Pope and Dockery, 2006). Thus, a number of

57   papers have shown that, based on size modality of PM and on composition size-

58   dependence, the combination of PM_{10} and PM_1 measurements is a good tool for air quality

59   monitoring (e.g. Morawska et al., 2008; Pérez et al., 2008). $PM_{2.5}$ measurements are widely

60   performed and used for source apportionment studies, however, the combination of PM_1

61   with PM_{10} is not so common. In particular, Perrone et al. (2013) highlighted the importance

62   of PM_1 measurements because it provides a better estimation of anthropogenic particles

63   than $PM_{2.5}$.

64 The concentration of PM at a specific location depends on a large number of factors, such

65 as local and regional PM sources as well as the meteorological conditions and geographical

66 situation. Thus, the design of strategies to reduce the concentrations of PM and meet the

67 European targets is a very difficult task. In this sense, several studies were conducted

68 during the past years in order to assess the main sources affecting PM concentration at

69 different environments by applying different methodologies. Receptor models, like Positive

70 Matrix Factorization (PMF, Paatero and Tapper, 1994), are widely used to identify the main

71 sources affecting PM from its chemical composition. Pant et al. (2012) remarked the need

72 of using size fractionated particulate matter in order to have an additional insight on aerosol

73 sources. However, there are only a few published works that use receptor models to identify

74 coarse aerosol sources separately from fine aerosol sources (e. g. Karanasiou et al., 2009;

75 Pandolfi et al., 2011; Minguillón et al., 2012). In addition, most source apportionment

76 studies are focused on sampling campaigns or short measurement periods (e. g. Minguillón

77 et al., 2012). The objective of this study is to assess the results obtained from source

78 apportionment analysis applied on chemical composition of size segregated data (coarse,

79 PM_{10-1}, and fine, PM_1, fractions) for an extended period of time (from 2006 to 2010). The

80 use of fine and coarse PM in the PMF analysis offers an additional insight into the sources

81 that may affect one of the size fractions and not the other. The exhaustive chemical

82 speciation and the quite long sampling period allow us for the identification of time trends

83 in PM concentration and sources. The study is focused in an urban environment where the

84 identification of sources contributing to PM is of great importance in order to establish

85 abatement strategies and meet the European requisites.

86 **2. Site and Methodology**

87   ## 2.1. Monitoring site

88   The measurements presented in this study were performed at Granada (37.18°N,

89   3.58°W, 680 m a.s.l), from 2006 to 2010. Granada is situated in the southeastern part of the

90   Iberian Peninsula and is a medium-sized city surrounded by mountains. Near continental

91   conditions are responsible for large seasonal temperature differences with most rainfall

92   occurring in spring and winter. The sampling site is located in the southern part of the city

93   and it is less than 500 metres away from a highway that surrounds the city.

94   ## 2.2. Chemical analyses

95   Simultaneous 24-hour samples (starting at 07:00 GMT) of PM_1 and PM_{10} were collected on

96   quartz fiber filters by means of two high-volume samplers (CAV-A/MSb and Digitel DHA-

97   80) with a flow rate of 30 m^3 h^{-1}. The PM_1 and PM_{10} daily samples were collected every

98   eight days from 2006 to 2010, except when failure of the instruments occurred. A total of

99   197 samples in PM_{10} and 163 in PM_1 were collected during the analysed period. The filters

100   were conditioned and treated pre- and post-sampling. The filters were placed in desiccators

101   during 48 hours prior to weighting at stabilized conditions (23°C and 50% RH) using

102   gravimetric techniques.

103   A complete chemical analysis was performed for all samples following the procedure of

104   Querol et al. (2001). A fraction of each filter was acid digested (HF HNO_3:$HClO_4$, 5:2.5:2.5

105   ml) and the resulting solution was used to determine major and trace elements by

106   Inductively Coupled Plasma Atomic Emission Spectrometry (ICP-AES) and Mass

107   Spectrometry (ICP-MS). Another portion of the filter was water leached with de-ionized

108   water in order to determine the concentration of Cl^-, SO_4^{2-} and NO_3^- by ion chromatography

109 and NH_4^+ mass concentration by colorimetry (Flow Injection Analysis). A third portion of

110 the filter was used to determine total carbon (Ct) content (Querol et al., 2013). From 2006

111 to July 2007 the total carbon mass concentration was determined using a LECO (Querol et

112 al., 2004), whilst since July 2007 the organic carbon (OC) and elemental carbon (EC) mass

113 concentrations were determined separately by means of a thermo-optical transmission

114 method using a Sunset Laboratory OCEC Analyser following the EUSAAR2 thermal

115 protocol (Cavalli et al., 2010). SiO_2 and CO_3^{2-} were indirectly determined on the basis of

116 empirical factors ($SiO_2 = 3$ x Al_2O_3 and $CO_3^{2-} = 1.5xCa$; Querol et al., 2004). Marine

117 sulfate ($SO_4^{2-}m$) concentration was calculated taking into account the Na/SO_4^{2-} molar ratio

118 determined for seawater (Drever, 1982). Non marine sulfate ($SO_4^{2-}nm$) was calculated as

119 the difference between total sulfate and marine sulfate. The non-mineral carbon (nmC) was

120 estimated by subtracting the C associated to carbonates from the total carbon content. PM_{10-1}

121 mass concentrations were calculated as the difference between PM_{10} and the

122 corresponding PM_1 mass concentrations. PM components were grouped as follows: mineral

123 (Σ Al_2O_3, SiO_2, CO_3, Ca, Fe, Mg, K), secondary inorganic aerosols, SIA, (Σ $SO_4^{2-}nm$, NO_3^-,

124 NH_4^+), salt (Σ Na, Cl, $SO_4^{2-}m$), OC, EC and trace elements (Σ Li, P, Sc, Ti, V, Cr, Mn, Co,

125 Ni, Cu, Zn, Ga, Ge, As, Se, Rb, Sr, Cd, Sn, Sb, Cs, Ba, La, Ce, Lu, Hf, Ta, W, Tl, Pb, Bi,

126 Th and U).

127   **2.3. Source apportionment method**

128 The chemical profiles of the potential sources affecting PM_{10-1} and PM_1 levels and their

129 contributions were identified by analyzing the PM_x composition data set with the Positive

130 Matrix Factorization model (PMF2; Paatero, 1997). The PM_1 matrix included 163 cases

131 and 24 variables whilst the PM_{10-1} matrix consisted of 130 cases and 22 variables. PMF

132 model is a factor analytical tool that provides the chemical profile and contribution of the

133 identified sources by solving the matrix problem $X = G \times F + E$ where X is the matrix of daily

134 chemical speciated data, G and F are the unknown matrixes of factor scores (source

135 contribution) and loading (source profile), respectively, and E is the matrix of residuals

136 (difference between measured and calculated species concentrations) (Paatero and Tapper,

137 1994; Paatero, 1997). The problem is solved by minimizing the objective function $Q = E/S$

138 where S is the matrix of the uncertainty in each data value. The minimization of Q is based

139 on the error-weighted least squares method, thus the calculation of the matrix S is a crucial

140 point so that the model gives the right weight to the input data and consequently the most

141 reliable results. In the present study, the matrix S for PM_1 and PM_{10} fractions was

142 calculated following the procedure described by Amato et al. (2009) and Escrig et al.

143 (2009) by propagating the uncertainties of the analytical procedures jointly with the

144 uncertainty related with the subtraction of the blank filters that are different filters from the

145 sampled ones. The applied formula gives higher relative errors for small concentration data

146 near the limit of detection. The uncertainties for the PM_{10-1} fractions were calculated by

147 propagating the errors calculated for the PM_1 and PM_{10} fractions with the above described

148 methodology. The number of species used within the PMF model was selected by looking

149 at their signal-to-noise ratio (S/N) which provides a criterion to separate the species which

150 retain a significant signal from the ones dominated by noise. The S/N was calculated as

151 described by Paatero and Hopke, (2003). Only species with S/N values higher than 2 were

152 selected for the present study, thus species with weak signal were not introduced in the

153 model (Paatero and Hopke, 2003). Moreover, the percentage of data above detection limit

154 (%ADL) was used as complementary criterion for species selection. The combination of

155 both criteria resulted in the selection of 24 species in PM_1 and 22 species in PM_{10-1}. Two

156 species (As and NH_4^+) were included in PM_1 and removed from PM_{10-1} given that these two

157 elements were found mainly in the finest fraction. In order to avoid bias in the results the

158 data matrix was uncensored, i.e. negative values and data below detection limits were

159 included as such in the analysis without substituting them with below detection limit

160 indicators (Paatero, 1997). Table S1 of the supplementary material reports means, standard

161 deviations, medians, percentage of data above detection limit (%ADL) and signal-to-noise

162 (S/N) for the selected elements. The PMF2 model was run in robust mode (Paatero, 1997)

163 for source identification and apportionment. The optimal number of sources was selected

164 by inspecting the variation of Q from PMF with varying number of sources (from 3 to 6)

165 and by studying the physical meaningfulness of the calculated factors. In the present work,

166 5 and 4 sources were selected for PM_{10-1} and PM_1, respectively. The theoretical value of Q

167 should be approximately equal to the number of degrees of freedom of the system

168 [$n{\times}m{-}(p{\times}(n{+}m))$] (Paatero et al., 2002) where n, m and p are the number of samples,

169 species and factors respectively. In PM_1 (with p=4) and PM_{10-1} (with p=5) the degrees of

170 freedom were 3356 and 2320, respectively, close to the calculated Q (3626 and 2586 for

171 PM_1 and PM_{10-1}, respectively). Moreover, in PM_1 and PM_{10-1} the solution with 5 and 6

172 factors, respectively, led to additional factors without a meaningful chemical profile both

173 being loaded with almost all used species. One additional criteria used to evaluate the

174 meaningfulness of the calculated sources was the inspection of the scaled residuals. In both

175 fractions the selected number of factors led to solutions with 90–100% of the scaled

176 residuals located between the optimal range −2 and +2 (Juntto and Paatero, 1994). Once the

177 number of sources was selected the rotational ambiguity was handled by means of the

178 Fpeak parameter by studying the variation in the Q values by varying Fpeak from −0.8 and

179 +0.8. Fpeak rotations were made in order to explore alternative solutions. The issue of local

180 minimum was assessed by running 20 times the Fpeak=0 solution with different

181 pseudorandom initializations. After regression of the factor scores from PMF (G matrix) to

182 PM mass the model was able to simulate on average 100% and 97 % of measured PM_{10-1}

183 and PM_1 mass, respectively, with coefficients of correlation of 0.97 (PM_{10-1}) and 0.75

184 (PM_1) (Figure S1).

185 **3. Results and discussion**

186   **3.1. PM concentration: major and trace elements**

187 Mean (± standard deviation) PM levels measured at Granada urban station for the entire

188 observation period 2006-2010 were 40 ± 30 μg/m^3 and 17 ± 9 μg/m^3 for PM_{10} and PM_1,

189 respectively. The chemical speciation obtained in this study was very similar to that

190 reported previously for the year 2006 (Titos et al., 2012). PM_{10-1} was mainly composed by

191 mineral matter (around 62%) and nmC (12%) whilst PM_1 was composed mainly by nmC

192 (32%) and SIA that contributed around 20%. Figure 1 shows the chemical speciation of

193 PM_{10-1} and PM_1 fractions during winter (November-February) and summer (May-August).

194 This separation can offer an insight in the possible sources and processes affecting coarse

195 and fine PM. Also the partitioning between PM_1 and PM_{10-1} (expressed through the ratio

196 PM_1/PM_{10}) can help to elucidate the origin of the elements analyzed (Figure 2). Mineral

197 matter was mainly in the coarse mode and its contribution to this fraction was higher in

198 summer than in winter (Figure 1). Figure 2 also evidences this fact; most of the crustal

199 elements presented low PM_1/PM_{10} ratios denoting that those elements are mainly in the

200 coarse fraction. The higher contribution of mineral matter to PM_{10-1} in summer can be due

201 to the drier conditions that favor re-suspension of dust from roads and soils as well as to the

202   dust intrusions from North Africa that are very frequent in Granada during summer season

203   (Valenzuela et al., 2012). The contribution of nmC to PM_1 fraction was higher than the

204   contribution to PM_{10-1} and also higher in winter than in summer. This seasonality of

205   carbonaceous material is typical of urban sites and may be due to the increase in

206   anthropogenic emissions (fuel based domestic heating) and lower mixing layer heights

207   during winter season (Granados-Muñoz et al., 2012) that favor accumulation of particles

208   near urban sources. In addition, during winter time, stagnant episodes associated with

209   thermal inversions and low wind speeds are also very frequent producing a large increase in

210   particle matter load near the ground (Lyamani et al., 2012).

211   **[Figure 1]**

212   Non marine sulfate was presented in both PM fractions, with slightly higher contribution in

213   PM_1 than in PM_{10-1}. This constituent doubled its contribution to PM_1 during summer due to

214   the higher SO_2 oxidation rates under high insolation conditions and low regional air mass

215   renovation in summer (Pey et al., 2009). On the contrary, nitrate contribution to PM_1

216   decreased considerably during summer due to the thermal instability of the ammonium

217   nitrate in summer (Harrison and Pio, 1983; Querol et al., 2008). Nitrate contribution to

218   PM_{10-1} did not vary significantly between seasons compared with its contribution to PM_1

219   and presented a PM_1/PM_{10} ratio around 0.56 in winter and 0.15 in summer denoting that in

220   summer nitrate was mainly in the coarse fraction whilst in winter was predominantly in the

221   fine one. Coarse nitrate is formed by interaction between HNO_3 and coarse marine (sodium

222   chloride) or mineral (calcium carbonate) particles giving rise to the formation of Na and/or

223   Ca nitrates explaining the higher concentrations of coarse nitrate observed in summer

224   (Tobo et al., 2010).

225 **[Figure 2]**

226   Most trace elements presented relatively low concentrations compared with the typical

227   values observed in other Spanish urban stations (Querol et al., 2008). Elements associated

228   with road traffic such as Cu and Sb (from brake abrasion; Schauer et al., 2006), Ba and Zn

229   (from tyre abrasion; Wahlin et al., 2006) and Ti, Li, and Rb, among others, from road

230   pavement abrasion (Querol et al., 2008; Amato et al., 2011) tended to accumulate in the

231   coarse fraction (50 to 90%). On the other hand, Ni presented a higher PM_1/PM_{10} ratio

232   ranging from 0.5 during winter to 0.7 in summer. Other elements associated with industrial

233   processes (As, Pb, Cd and U; Querol et al., 2008) mostly accumulate in the fine fraction.

234   Most elements presented higher PM_1/PM_{10} ratios during winter compared with summer,

235   except Bi, Sn, V, Ni and EC. A different seasonality in the PM_1/PM_{10} ratio may suggest

236   differences in the sources contributing to these compounds in winter and in summer (see

237   next section). A similar seasonal behavior for the PM_1/PM_{10} ratios for Ni, Sn, EC and V

238   was also observed in Switzerland by Minguillón et al. (2012).

239   Mean PM_{10} annual levels decreased from 50 ± 30 μg/m^3 in 2006 to 40 ± 30 μg/m^3 in 2010.

240   Meteorological conditions and emissions are competitive processes determining the

241   magnitude of PM concentrations in the atmosphere. Thus, the year to year variability

242   observed in PM_{10} levels could be related to inter-annual variations in emissions sources or

243   to changes in the meteorological and synoptic conditions, or to both. In order to detect

244   possible trends in PM_{10} and PM_1 component levels, the Mann-Kendall test has been applied

245   to the annual average values. This test reveals a significant decreasing trend (at 0.1

246   significance level) in PM_{10} and mineral matter concentrations. Saharan dust intrusions over

247   Granada have a large impact on the PM_{10} and PM_1 levels and their constituents (Calvo et

248   al., 2010; Mladenov et al., 2011). Thus, part of the observed year to year variations in PM_{10}

249   and PM_1 component levels could be due to the inter-annual variation in the frequency and

250   intensity of Saharan dust events. In order to discard the variability caused by African dust

251   events, the samples collected under those conditions have been excluded. A total of 134

252   PM_{10} samples were collected under African dust free conditions (www.calima.ws). Under

253   these conditions, significant decreasing trends at 0.05 significance level were obtained for

254   PM_{10} mass concentration, mineral matter, nmC and V and at 0.1 significance level for SIA,

255   Cu and Pb. No trends were obtained for trace elements such as Ni, Sn, Sb, Co, Zn or Cr.

256   Lyamani et al. (2011) reported that equivalent black carbon mass concentrations decreased

257   on 2008 due to the decrease in anthropogenic activities in Granada. The current work

258   shows that this decrease has continued until 2010 and that other anthropogenic pollutants

259   have also decreased. On the other hand, annual PM_1 levels did not experience any

260   significant temporal trend according to the Mann-Kendall test. Recent studies of

261   Barmpadimos et al. (2012) and Cusack et al. (2012) have reported a decreasing trend in

262    $PM_{2.5}$ levels at regional stations across Europe for the periods 1998-2010 and 2002-2010,

263   respectively. In the study of Barmpadimos et al. (2012) the decrease observed in $PM_{2.5}$ was

264   more pronounced than the decrease observed for PM_{10} levels. However, in Granada, the

265   decrease was mainly observed in the PM_{10} fraction. This discrepancy could be ascribed to

266   different sampling sites between studies (regional versus urban) and to different size

267   fractions ($PM_{2.5}$ versus PM_1). Thus, we believe that the observed decrease in PM_{10} and its

268   constituents may be related, in large part, to a decrease in the anthropogenic activities

269   although part of the observed decrease may be also due to the inter-annual change in the

270   meteorological conditions.

271   **3.2. Apportionment and seasonality of the sources identified by PMF.**

272   Five PM_{10-1} and four PM_1 sources were identified by PMF analysis. Figure 3 and Figure 4

273   show the profiles of each source in the coarse and fine fractions, respectively, and the

274   percentages of species apportioned by each source. The sources identified in the coarse

275   fraction were named as mineral dust, regional re-circulation, aged regional, road dust and

276   celestite mines. Fine PM sources were mineral dust, regional re-circulation, traffic exhaust

277   and road dust. Although some sources were identified in both fractions the use of fine and

278   coarse PM in the PMF analysis allows for the identification of additional sources.

279   *- Mineral dust*

280   The mineral source was identified in both fractions and was characterized by crustal

281   elements (Al_2O_3, Ca, Mg, Fe, Ti, Sr). This source might have contribution of both local (re-

282   suspension from soils and construction activities) and long-range transported dust aerosols.

283   It comprised 36 and 22% of the total mass in the coarse and fine fractions, respectively. It is

284   necessary to highlight the high contribution of this source to the fine fraction since mineral

285   matter commonly accumulates in the coarse fraction (Song et al., 2012). Some authors

286   (Minguillón et al., 2012; Perrone et al., 2013; Cusack et al., 2013) have identified mineral

287   sources by applying PMF. However, none of them reported such high contributions to the

288   fine fraction. This high contribution to the fine fraction may be ascribed to contamination

289   of the source profile although the profile was not cleaner for other Fpeak values. The

290   presence of SO_4^{2-} and C in the mineral PM_1 profile could be due to: 1) Neutralization of

291   sulfuric acid with available ions such as Ca^{++} and Na^+ (also present in the mineral PM_1

292   profile) and 2) Contamination by C due to condensations of organic precursors on large

293 surface mineral particles. Using PMF analysis the contribution of mineral matter doubled

294 the contribution calculated as Σ Al_2O_3, SiO_2, CO_3, Ca, Fe, Mg, K. Concerning the

295 seasonality of this source, it showed a higher contribution to PM in summer than in winter

296 probably connected with the higher frequency of African dust events during spring and

297 summer and with the dryness of the soil which favor re-suspension processes.

298 *- Road dust*

299 The road dust source was slightly different for each size fraction. In PM_1 it was mainly

300 characterized by carbonaceous particles and Sb (90% of the total variance of Sb) whereas in

301 the coarse fraction it was typified by carbonaceous material and road tracers like Fe, Cu,

302 Sn, Sb and Pb (Amato et al., 2009). This source was predominantly in the coarse fraction,

303 comprising 8% and 24% of the total fine and coarse PM, respectively. It presented a similar

304 seasonality in both fractions with higher contribution to the coarse and fine mass in winter

305 (48% and 11%, respectively) with respect to summer (12% and 7%, respectively) (Figure

306 5). The interpretation of this source is supported by the polar plots, since higher

307 concentrations (Figure S3) were obtained for low wind speeds and for southwesterly winds

308 (in the direction of the highway). A similar contribution of road dust to PM_{10} was obtained

309 in a traffic oriented site located in the northern part of the city (Amato et al., 2013).

310 *-Traffic exhaust*

311 This source was only identified in the fine fraction and it was characterized by nitrate,

312 ammonium and carbonaceous particles, comprising 29% of the fine mass. This source

313 explained 86% of variance in nitrate that in urban environments is mainly attributed to

314 vehicle exhaust (Almeida et al., 2006). The presence of some road tracers confirms the

315   traffic origin of this source. The higher contribution in winter can be connected with higher

316   emissions together with lower mixing layer heights (Granados-Muñoz et al., 2012) that

317   favor accumulation of pollutants near the surface. In addition, fine nitrate concentrations

318   could increase in winter due to the thermal stability of particulate nitrate. In this sense, it is

319   important to have in mind that the formation of secondary products from primary emissions

320   depends on the season and that primary products are not always transformed into the same

321   compounds in the atmosphere. The polar plots (Figure S3) and the seasonality of this

322   source and the road dust source are very similar, confirming a common source.

323   *- Regional re-circulation*

324   This source is traced by secondary sulfate (mainly in the form of ammonium sulfate), V and

325   Ni. It is the most important source concerning PM_1 mass concentration, comprising 41% of

326   the total mass in this fraction. Secondary sulfate, V and Ni are commonly associated with

327   fuel-oil combustion and used as tracers for domestic heating and traffic sources (e.g. Calvo

328   et al., 2013). In addition, high concentrations of V, Ni and sulfate, especially during

329   summer season, are commonly reported in Mediterranean environments associated with re-

330   circulation processes (Pey et al., 2013). The seasonality of the regional re-circulation source

331   (Figure 5) with higher contribution in summer (9.5 $\mu g/m^3$ in PM_1 and 2.0 $\mu g/m^3$ in PM_{10-1})

332   compared to winter (4.0 $\mu g/m^3$ and 1.1 $\mu g/m^3$ in PM_1 and PM_{10-1}, respectively) suggests

333   that an important part of this source may be ascribed to regional pollution and long range

334   transport, especially in summer, although in winter it may be ascribed to domestic heating,

335   being the PMF analysis unable to distinguish between both sources. In this sense, also the

336   variations in the PM_1/PM_{10} ratios of V and Ni in summer and winter (Figure 2) evidence

337   differences in the sources contributing to these compounds depending on the season.

338   *- Aged regional*

339   This source was typified by nitrate, sulfate, Na, Cl, Se and Ct, and has been interpreted as

340   aged regional, being only identified in the coarse fraction. Its seasonality is characterized

341   by a relatively high contribution during the warm season (14%, 5.5 $\mu g/m^3$) compared with

342   winter (12%, 2.4 $\mu g/m^3$). It is thought to be related with the interaction of secondary

343   compounds (sulfates and nitrates) with mineral matter and marine aerosols. Regional re-

344   circulation processes together with Saharan dust intrusions (both more frequent in summer

345   season) may favor this interaction. In fact, the presence of coarse nitrate in this source (62%

346   of the variance) is thought to be related with the aforementioned formation of $Ca(NO_3)_2$

347   during dust events due to the interaction of mineral dust with anthropogenic pollutants

348   (Tobo et al., 2010).

349   *- Celestite mines*

350   The main tracers of this source were sulfate, strontium and crustal elements (mainly Ca and

351   Mg). It was named as celestite mines because it was thought to be related with celestite

352   mines located 20 km south-west of the city. Celestite ($SrSO_4$) is a mineral consisting of

353   strontium sulfate and is the principal source of the element strontium, commonly used in

354   fireworks and in various metal alloys. This source was only distinguished in the coarse

355   fraction and its mass contribution to this fraction was 20%. This source displayed a

356   seasonal pattern characterized by higher values in summer compared with winter, which

357   could be explained since the mines are open-pit mines, so re-suspension is enhanced during

358   summer. In addition, the fields surrounding the mines would be enriched in Sr, thus

359   agricultural activities in the area will also favor re-suspension of this element. The highest

360 concentration of this source was obtained for westerly and south-westerly winds, where the

361 mines are located (Figure S3) although relatively high concentrations were also observed

362 for winds from the east sector. This may be due to the contribution of other mineral

363 compounds to this source as can be seen in Figure 3.

364 **[Figure 3]**

365 **[Figure 4]**

366 **[Figure 5]**

367 **3.3. Working versus non-working days variability**

368 The average contribution of the different sources for working days (from Monday to

369 Friday), Saturday and Sunday is shown in Figure 6. For the coarse fraction a total of 92

370 data points are included in the average for Monday-Friday, 20 for Saturday and 18 for

371 Sunday. In a similar manner for the fine fraction 119, 25 and 19 data points are included in

372 the averages for Monday-Friday, Saturday and Sunday, respectively. It is important to take

373 into account the sampling interval of the filters (24 hours starting at 7:00 GMT). In

374 particular, filters collected on Sunday include partially the traffic peak of Monday morning.

375 PM_{10-1} experienced a large decrease from weekdays (31 ± 23 μg/m^3) to Saturdays (20 ± 10

376 μg/m^3), showing also less variability on Saturdays. On Sundays, the average PM_{10-1} mass

377 concentration increase compared to Saturdays, probably due to the traffic peak of Monday

378 mornings. The largest decrease was observed for the mineral dust source that decreased

379 from an average value of 11 ± 7 μg/m^3 on Monday-Friday to 5 ± 4 μg/m^3 on Saturdays.

380 Celestite mines source also decreased considerably on Saturdays, denoting a reduction in

381 the working activity of the mines during the weekend. Taking into account the standard

382 deviations, the decrease observed in the contributions of the celestite mines source was

383 more pronounced than in the mineral dust source. Road dust source experienced a slight

384 decrease during the weekend whilst regional re-circulation and aged regional sources did

385 not change significantly from weekdays to weekends. Concerning the fine fraction, PM_1

386 levels did not vary between weekdays and weekends. It is necessary to mention that part of

387 the variability between working and non-working days may be biased by the lower number

388 of samples collected during Saturdays and Sundays.

389   **[Figure 6]**

390 So, reducing anthropogenic activity (like it is supposed to occur on Saturdays) will have a

391 positive impact in PM_{10} levels. However, in the short term the reduction observed occurred

392 mainly in the coarse fraction, whereas the fine fraction remains at the same levels during

393 the weekends.

394 **3.4. Daily exceedances: natural or anthropogenic?**

395 Air quality has been a cause of concern during the past decades throughout the world,

396 especially in developed countries. In particular, PM has become a key pollutant due to its

397 negative effects on human health and many countries have developed abatement strategies

398 in order to control PM levels. Therefore, one of the main aims of source apportionment

399 studies is to identify the causes of exceedance of the thresholds established by the European

400 Directive (2008/50/EC for PM_{10} and $PM_{2.5}$; no regulation concerning PM_1). A total of 40

401 PM_{10} daily exceedances have been recorded during the study period, with most of them

402 occurring during spring and summer seasons (15 and 12, respectively). From the 27 daily

403   exceedances, 22 occurred during African dust events (www.calima.ws). On average, the

404   ratio fine/coarse mass concentration was 0.5 during the exceedances occurred in spring and

405   summer and the mineral dust source accounted for 24% of the measured PM_1 and 48% of

406   PM_{10-1}. For days exceeding the PM_{10} daily limit during autumn and winter, road dust and

407   mineral dust sources comprised 42 and 29% of the coarse fraction; and traffic exhaust and

408   regional re-circulation accounted for 55% and 23% of the total PM_1, respectively. The

409   fine/coarse ratio was on average 0.9, during those days. Thus, exceedances associated with

410   a natural origin were more frequent during spring and summer and presented a higher

411   impact on the coarse fraction. On the other hand, exceedances related to an anthropogenic

412   origin predominantly affected the fine fraction and occurred more often during the cold

413   seasons. With these results in mind, traffic is the main source to target in Granada

414   throughout the year, but especially in winter. In this sense, Qadir et al. (2013) detected a

415   decrease of 60% in the contribution of traffic source after the implementation of a low

416   emission zone in Munich, evidence that this kind of measurements may help to reduce

417   pollution levels in urban areas.

418   **4. Conclusions**

419   The chemical composition of fine and coarse particulate matter has been studied for the

420   period 2006-2010 at an urban station in southern Iberian Peninsula. A significant

421   decreasing trend in PM_{10} levels has been observed related with a decrease in most of its

422   constituents, specially marked in mineral matter levels and nmC. The concentrations of

423   chemical constituents were found to undergo a clear seasonal behavior. The coarse fraction

424   was mainly composed by mineral matter, which increased considerably during summer due

425   to the drier conditions that favor re-suspension from roads and soils and the more frequency

426   of African dust events. Non-mineral carbon was the major contributor to the fine fraction

427   and presented higher levels in winter than in summer mainly due to larger emissions during

428   winter and lower mixing layer heights that favor accumulation of particles near surface.

429   Concerning the identification of sources, PMF analysis distinguished five sources in PM_{10-1}

430   and four in PM_1. The use of fine and coarse PM in the PMF analysis allows the

431   identification of additional sources that could not be identified using only one size fraction.

432   The mineral dust source was identified in both fractions and comprised 36 and 22% of the

433   total mass in the coarse and fine fractions, respectively. This high contribution of the

434   mineral source to the fine fraction may be due to contamination of the source profile. The

435   regional re-circulation source was traced by secondary sulfate, V and Ni. It was the most

436   important source concerning PM_1 mass concentration being less important in the coarse

437   fraction. Although V and Ni are commonly associated to fuel oil combustion the

438   seasonality of this source with higher concentrations in summer compared with winter

439   suggest that the most important part of this source can be ascribed to regional pollution

440   episodes. The traffic exhaust source that was characterized by nitrate, ammonium and

441   carbonaceous particles, comprising 29% of the fine mass. Finally, celestite mines source

442   was traced by sulfate, strontium and crustal elements (mainly Ca and Mg) and it was only

443   identified in the coarse fraction.

444   A reduction in PM_{10-1} levels from working versus non-working days has been observed,

445   especially in mineral dust, celestite mines and road dust sources. On the other hand, PM_1

446   levels remain fairly constant throughout the week. PM_{10} exceedances (2008/50/EC)

447   associated with a natural origin were more frequent during spring and summer and

448   presented a higher impact on the coarse fraction, whereas exceedances related to

449   anthropogenic origin predominantly affected the fine fraction and occurred more often

450   during the cold seasons. Concluding, traffic seems to be the main source to target in

451   Granada throughout the year, but especially in winter. Since no significant temporal trend

452   or changes between working and non-working days have been observed in the fine fraction,

453   it is clear that further investigation is needed concerning PM_1 fraction and its sources in

454   order to establish future abatement strategies.

465

466

467

468

469

References

Almeida, S.M., Pio, C.A., Freitas, M.C., Reis, M.A., Trancoso, M.A., 2006. Source apportionment of atmospheric urban aerosol based on weekdays/weekend variability: evaluation of road re-suspended dust contribution. Atmos. Environ., 40, 2058-2067.

Amato, F., Pandolfi, M., Escrig, A., Querol, X., Alastuey, A., Pey, J., et al., 2009. Quantifying road dust resuspension in urban environment by multilinear engine: a comparison with PMF2. Atmos. Environ., 43 (17), 2770-2780.

Amato, F., Pandolfi, M., Moreno, T., Furger, M., Pey, J., Alastuey, A., et al., 2011. Sources and variability of inhalable road dust particles in three European cities. Atmos. Environ., 45, 6777-6787.

Amato, F., Alastuey, A., de la Rosa, J., González-Castanedo, Y., Sánchez de la Campa, A.M., Pandolfi, M., et al., 2013. Trends of road dust emissions contributions on ambient PM levels at rural, urban and industrial sites in Southern Spain. Atmos. Chem. Phys. Discuss., 13, 31933-31963.

Barmpadimos, I., Keller, J., Oderbolz, D., Hueglin, C., Prévôt, ASH., 2012. One decade of parallel fine (PM2.5) and coarse (PM10-PM2.5) particulate matter measurements in Europe: trends and variability. Atmos. Chem. Phys., 12, 3189-3203.

Calvo, A.I., Olmo, F.J., Lyamani, H., Alados-Arboledas, L., Castro, A., Fernández-Raga M., Fraile, R., 2010. Chemical composition of wet precipitation at the background EMEP station in Víznar (Granada, Spain) (2002-2006). Atmos. Res., 96, 2-3. 408-420.

490   Calvo, A.I., Alves, C., Castro, A., Pont, V., Vicente, A.M., Fraile, R., 2013.

491   Research on aerosol sources and chemical composition: Past, current and emerging issues.

492   Atmos. Res., 120-121, 1-28.

493   Cavalli, F., Viana, M., Yttri, K.E., Genberg, J., Putaud, J.P., 2010. Toward a

494   standardized thermal-optical protocol for measuring atmospheric organic and elemental

495   carbon: the EUSAAR protocol. Atmos. Meas. Tech., 3-1, 78-89.

496   Cusack, M., Alastuey, A., Pérez, N., Pey, J., Querol, X., 2012. Trends of particulate

497   matter (PM2.5) and chemical composition at a regional background site in the Western

498   Mediterranean over the last nine years (2002-2010). Atmos. Chem. Phys., 12, 8341-8357.

499   Cusack, M., Pérez, N., Pey, J., Alastuey, A., Querol, X., 2013. Source

500   apportionment of fine PM and sub-micron particle number concentrations at a regional

501   background site in the western Mediterranean: a 2.5 year study. Atmos. Chem. Phys., 13,

502   5173-5187.

503   Drever, J.J., 1982. The Geochemistry of Natural Waters. Prentice-Hall Inc,

504   Englewood Cliffs, NJ, 437pp.

505   Escrig, A., Monfort, E., Celades, I., Querol, X., Amato, F., Minguillón, M.C., et al.,

506   2009. Application of optimally scaled target factor analysis for assessing source

507   contribution of ambient PM10, J Air Waste Manag Assoc.,59(11), 1296-307.

508   Forster, P., Ramaswamy, V., Artaxo, P., Benstsen, T., Betts, R., Fahey, D.W., et al.,

509   2007. Changes in Atmospheric Constituents and in Radiative Forcing. In: Climate Change

510   2007: The Physical Science Basis. Contribution of Working Group I to the Fourth

511 Assessment Report of the Intergovernmental Panel on Climate Change [Solomon, S., Qin,

512 D., Mannning, M., Chen, Z., Marquis, M., Averyt, K.B., Tignor, M., and Miller, H.L.,

513 (eds)]. Cambridge University Press. Cambridge. United Kindom and New York, NY, USA.

514   Granados-Muñoz, M.J., Navas-Guzmán, F., Bravo-Aranda, J.A., Guerrero-Rascado,

515 J.L., Lyamani, H., Fernández-Gálvez, J., et al., 2012. Automatic determination of the

516 planetary boundary layer height using lidar: One-year analysis over southeastern Spain, J.

517 Geophys. Res., 117, D18208, doi:10.1029/2012JD017524.

518   Harrison, R.M., Pio, C., 1983. Size diferentiated composition of inorganic aerosol

519 of both marine and polluted continental origin. Atmos. Environ., 17, 1733-1738.

520   Juntto, S., Paatero, P., 1994. Analysis of daily precipitation data by positive matrix

521 factorization, Environmetrics, 5, 127–144.

522   Karanasiou, A.A., Siskos, P.A., Eleftheriadis, K., 2009. Assessment of source

523 apportionment by Positive Matrix Factorization analysis on fine and coarse urban aerosol

524 size fractions, Atmos. Environ., 43, 3385-3395.

525   Lyamani, H., Olmo, F.J., Foyo, I., Alados-Arboledas, L., 2011. Black carbon

526 aerosols over an urban area in south-eastern Spain: Changes detected after the 2008

527 economic crisis. Atmos. Environ., 45, 6423-6432.

528   Lyamani, H., Fernández-Gálvez, J., Pérez-Ramírez, D., Valenzuela, A., Antón, M.,

529 Alados, I., et al., 2012. Aerosol properties over two urban sites in South Spain during an

530 extended stagnation episode in winter season. Atmos. Environ., 62, 424-432.

531   Minguillón, M.C., Querol, X., Baltensperger, U., Prévôt, A.S.H., 2012. Fine and

532   coarse PM composition and sources in rural and urban sites in Switzerland: Local or

533   regional pollution?. Sci. Total. Environ., 427-428, 191-202.

534   Mladenov, N., Alados-Arboledas, L., Olmo, F.J., Lyamani, H., Delgado, A.,

535   Molina, A., Reche, I., 2011. Applications of optical spectroscopy and stable isotope

536   analyses to organic aerosol source discrimination in an urban area. Atmos. Environ., 45, 11,

537   1960-1969.

538   Morawska, L., Keogh, D.U., Thomas, S.B., Mengersen, K., 2008. Modality in

539   ambient particle size distributions and its potential as a basis for developing air quality

540   regulation. Atmos. Environ., 42, 1617-1628.

541   Paatero, P., Tapper, U., 1994. Positive matrix factorization: a nonnegative factor

542   model with optimal utilization of error estimates of data values, Environmetrics, 5, 111–

543   126.

544   Paatero, P., 1997. Least square formulation of robust non-negative factor analysis,

545   Chemometr. Intell. Lab. Syst., 3, 23–35.

546   Paatero, P., Hopke, P.K., Song, X., and Ramadan, Z., 2002. Understanding and

547   controlling rotations in factor analytic models, Chemo metrics and Intelligent Laboratory

548   Systems, 60(1–2), 253–264.

549   Paatero, P., Hopke, P. K., 2003. Discarding or downweighting high noise variables

550   in factor analytic models, Anal Chim Acta, 490, 277–289.

551   Pandolfi, M., Gonzalez-Castanedo, Y., Alastuey, A., de la Rosa, J., Mantilla, E.,

552   Sanchez de la Campa, A., et al., 2011. Source apportionment of PM10 and PM2.5 at

553   multiple sites in the Straits of Gibraltar by PMF: impact of shipping emissions. Environ.

554   Sci. Pollut. Res., 18:260-269.

555   Pant, P., Harrison, R.M., 2012. Critical review of receptor modeling for particulate

556   matter: A case study of India. Atmos. Environ., 49, 1-12.

557   Pérez, N., Pey, J.,   Querol, X., Alastuey, A., López, J.M., Viana, M., 2008.

558   Partitioning of major and trace components in PM10-PM2.5-PM1 at an urban site in

559   Southern Europe. Atmos. Environ., 42, 1677-1691.

560   Perrone, M.R., Becagli, S., García-Orza, J.A., Vecchi, R., Dinoi, A., Udisti, R.,

561   Cabello, M., 2013. The impact of long-range-transport on PM1 and PM2.5 at a Central

562   Mediterranean site. Atmos. Environ., 71, 176-186.

563   Pey, J., Pérez, N., Castillo, S., Viana, M., Moreno, T., Pandolfi, M., et al., 2009.

564   Geochemistry of regional background aerosols in the Western Mediterranean. Atmos. Res.,

565   94, 422-435.

566   Pey, J., Alastuey, A., Querol, X., 2013. PM10 and PM2.5 sources at an insular

567   location in the western Mediterranean by using source apportionment techniques. Sci.

568   Total. Environ., 456-457, 267-277.

569   Pope, C.A., Dockery, D.W., 2006. Health effects of fine particulate air pollution:

570   lines that connect. J Air Waste Manage Assoc; 56:709–42.

571   Qadir, R.M., Abbaszade, G., Schnelle-Kreis, J., Chow, J.C., Zimmermann, R.,

572 2013. Concentrations and source contributions of particulate organic matter before and after

573 implementation of a low emission zone in Munich, Germany. Environmental Pollution,

574 175, 158-167.

575   Querol, X., Alastuey, A., Rodriguez, S., Plana, F., Ruiz, C.R., Cots, N., et al., 2001.

576 PM10 and PM2.5 source apportionment in the Barcelona Metropolitan area, Catalonia,

577 Spain. Atmos. Environ., 35, 6407-6419.

578   Querol, X., Alastuey, A., Viana, M., Rodriguez, S., Artiñano, B., Salvador, P., et al.,

579 2004. Speciation and origin of PM10 and PM2.5 in Spain, J. Aerosol Sci., 35, 1151–1172.

580   Querol, X., Alastuey, A., Moreno, T., Viana, M.M., Castillo, S., Pey, J., et al., 2008.

581 Spatial and temporal variations in airborne particulate matter (PM10 and PM2.5) across

582 Spain 1999–2005, Atmos. Environ., 42:3964–3979.

583   Querol, X., Alastuey, A., Viana, M., Moreno, T., Reche, C., Minguillon, M.C., et

584 al., 2013. Variability of carbonaceous aerosols in remote, rural, urban and industrial

585 environments in Spain: implications for air quality policy, Atmos. Chem. Phys., 13, 6185–

586 6206.

587   Schauer, J.J., Lough, G.C., Shafer, M.M., Christensen, W.F., Arndt, M.F.,

588 DeMinter, J.T., 2006. Characterization of metals emitted from motor vehicles. Health

589 Effects Institute.

590   Song, S., Wu, Y., Jiang, J., Yang, L., Cheng, Y., Hao, J., 2012. Chemical

591   characteristics of size-resolved PM2.5 at a roadside environment in Beijing, China.

592   Environmental Pollution, 161, 215-221.

593   Titos, G., Foyo-Moreno, I., Lyamani, H., Querol, X., Alastuey, A., Alados-

594   Arboledas, L., 2012. Optical properties and chemical composition of aerosol particles at an

595   urban location: An estimation of the aerosol mass scattering and absorption efficiencies, J.

596   Geophys. Res., 117, D04206, doi:10.1029/2011JD016671.

597   Tobo, Y., Zhang, D., Matsuki, A., Iwasaka, Y., 2010. Asian dust particles converted

598   into aqueous droplets under remote marine atmospheric conditions. PNAS, 107(42):

599   17905–17910.

600   Valenzuela, A., Olmo, F.J., Lyamani, H., Antón, M., Quirantes, A., Alados-

601   Arboledas, L., 2012. Analysis of the desert dust radiative properties over Granada using

602   principal plane sky radiances and spheroids retrieval procedure. Atmos. Res., 104-105,

603   292–301.

604   Wahlin, P., Berkowicz, R., Palmgren, F., 2006. Characterization of traffic-generated

605   particulate matter in Copenhagen. Atmos. Environ., 40, 2151-2159.

606

607

608

609

610 **Figures captions**

611 **Figure 1:** Chemical composition of PM_{10-1} (lower panel) and PM_1 (upper panel) in winter

612 and in summer expressed in $\mu g/m^3$ and percentage (%).

613 **Figure 2:** PM_1/PM_{10} ratios of the major and some trace elements.

614 **Figure 3:** Source profiles found for the coarse fraction (PM_{10-1}) and percentage of ambient

615 species concentration apportioned by each source.

616 **Figure 4:** Source profiles found for the fine fraction (PM_1) and percentage of ambient

617 species concentration apportioned by each source.

618 **Figure 5:** Contribution of sources to PM_{10-1} (upper panel) and PM_1 (lower pannel) in winter

619 (left) and summer (right) expressed in $\mu g/m^3$ and corresponding percentage.

620 **Figure 6:** Average concentrations of each source for Monday to Friday, Saturday and

621 Sunday, for the coarse fraction (upper panel) and for the fine fraction (lower panel). The

622 error bars represent the standard deviations (SD). The average $\pm$ SD measured PM mass

623 concentration for each period is also shown in a box.

624

625

626

627

628

629 **Figure 1**
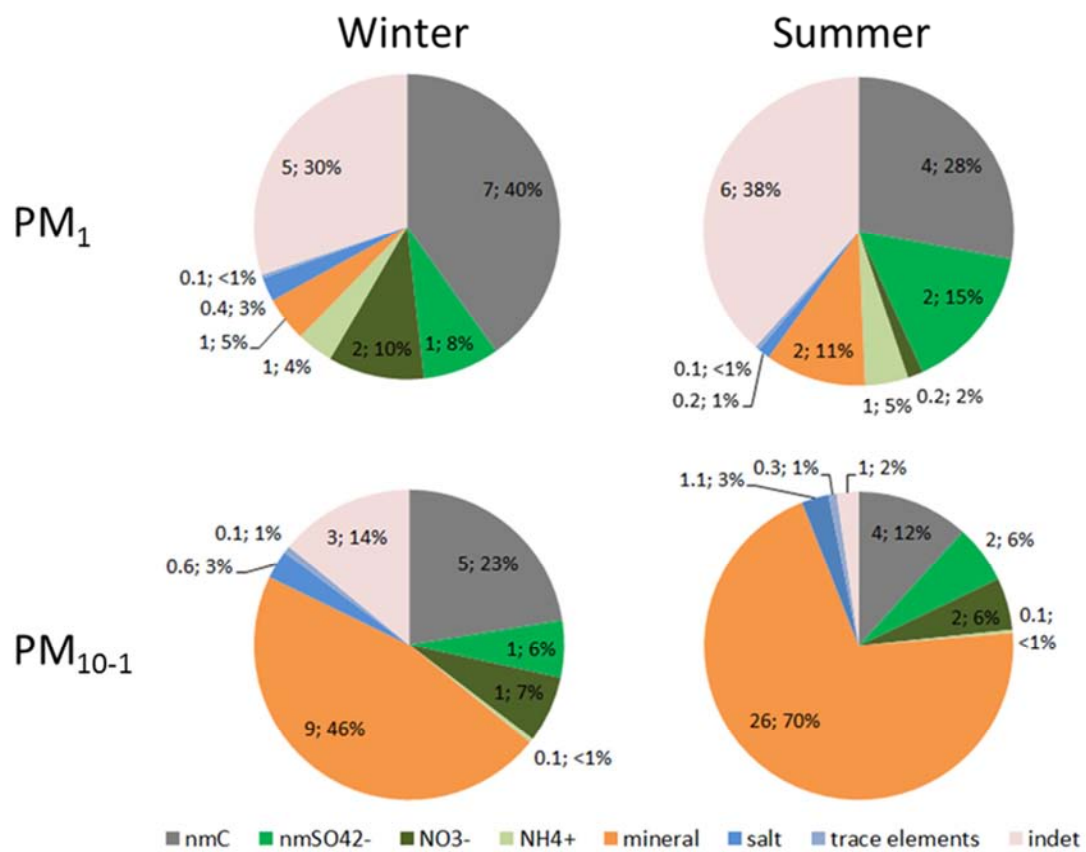
630

631

632

633

634

635

636

637   **Figure 2**
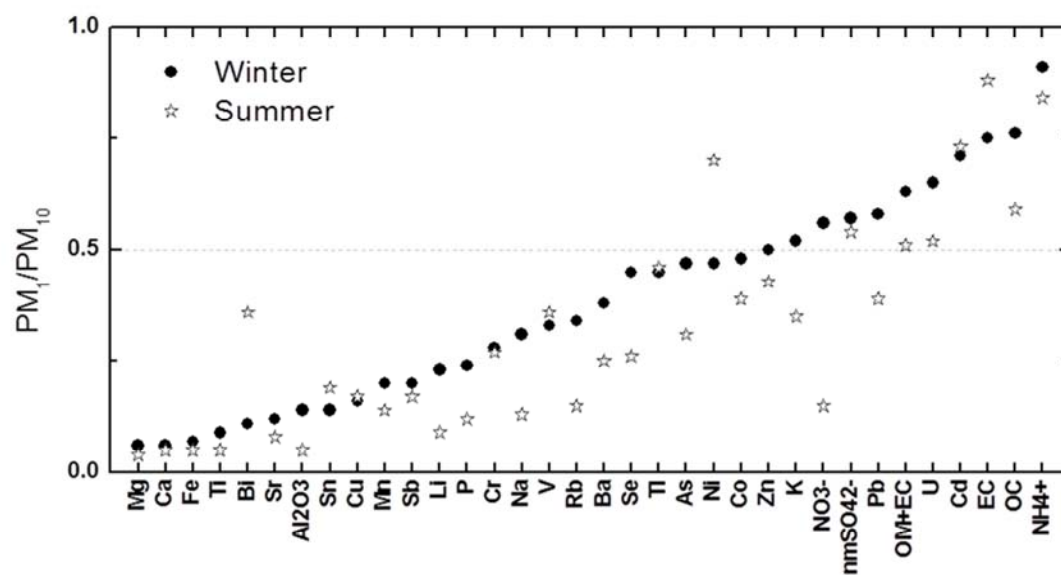
638

639

640

641

642

643

644

645

646

647

648   **Figure 3**
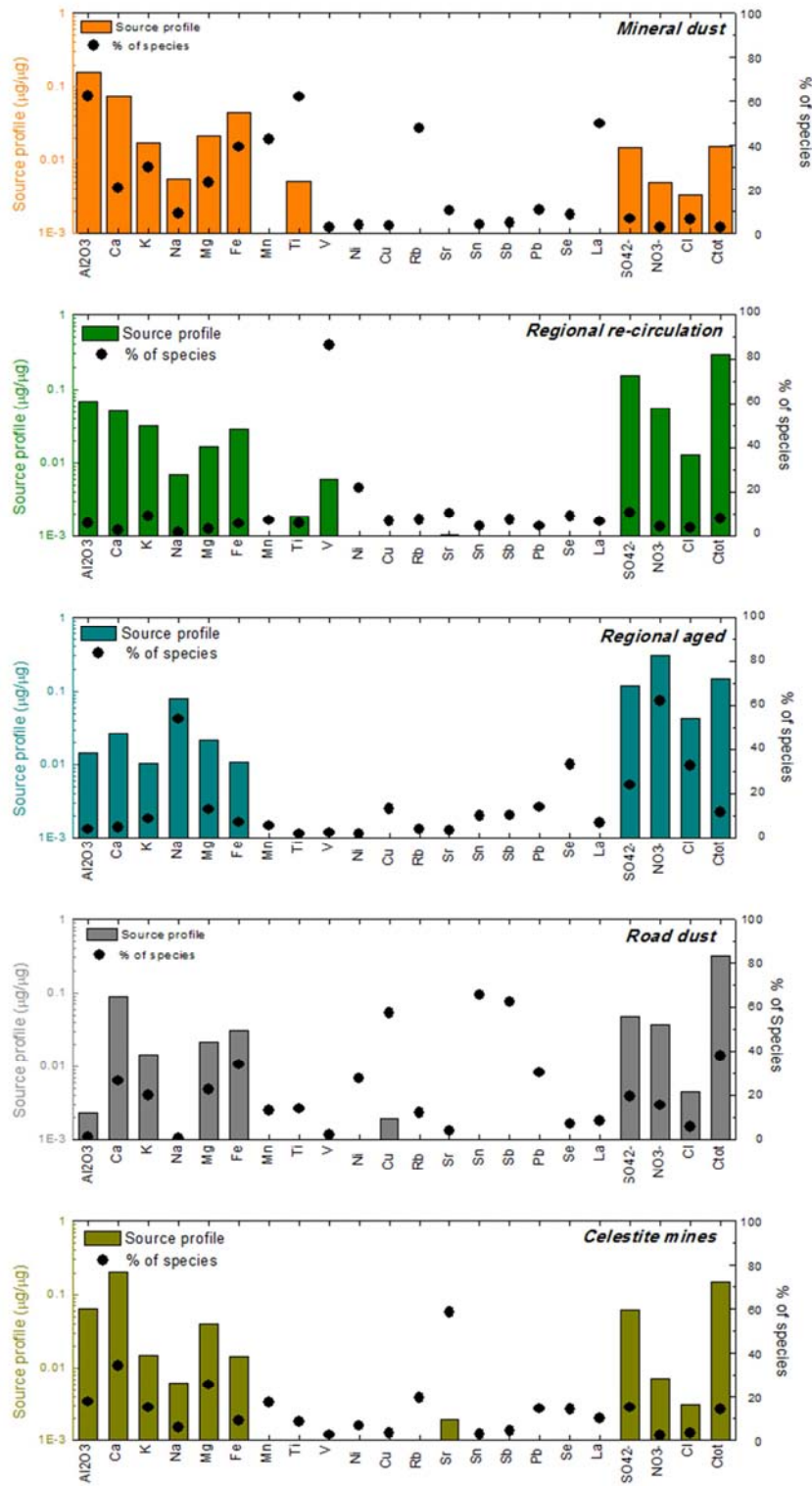
649

650   **Figure 4**
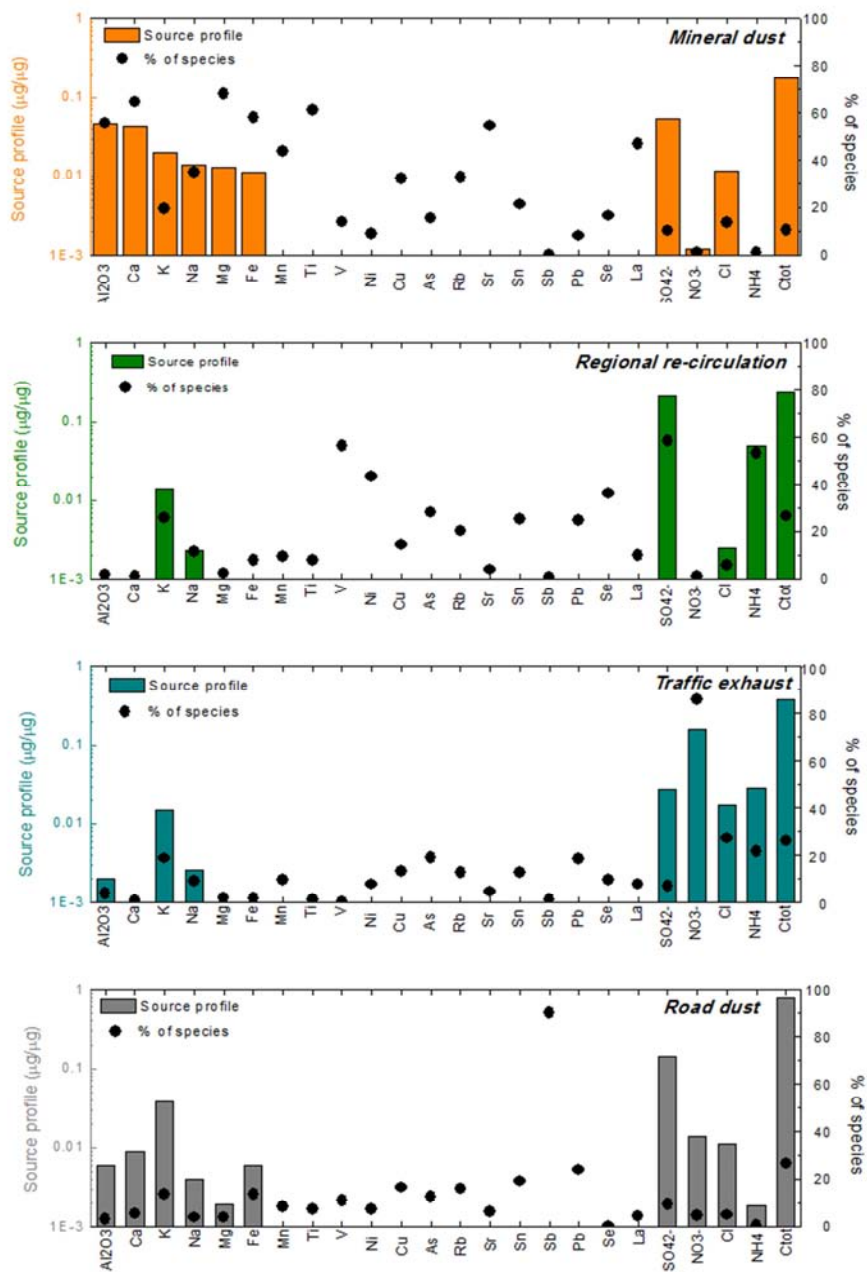
651

652

653

654 **Figure 5**
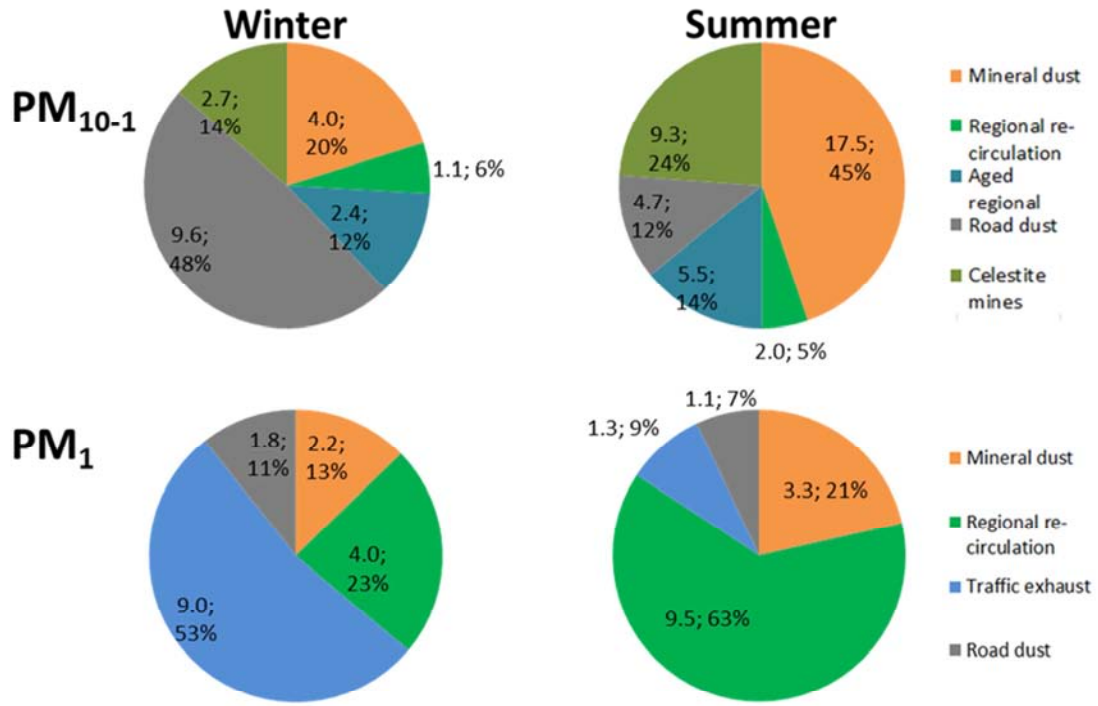
655

656

657

658

659

660

661

662

663 **Figure 6**
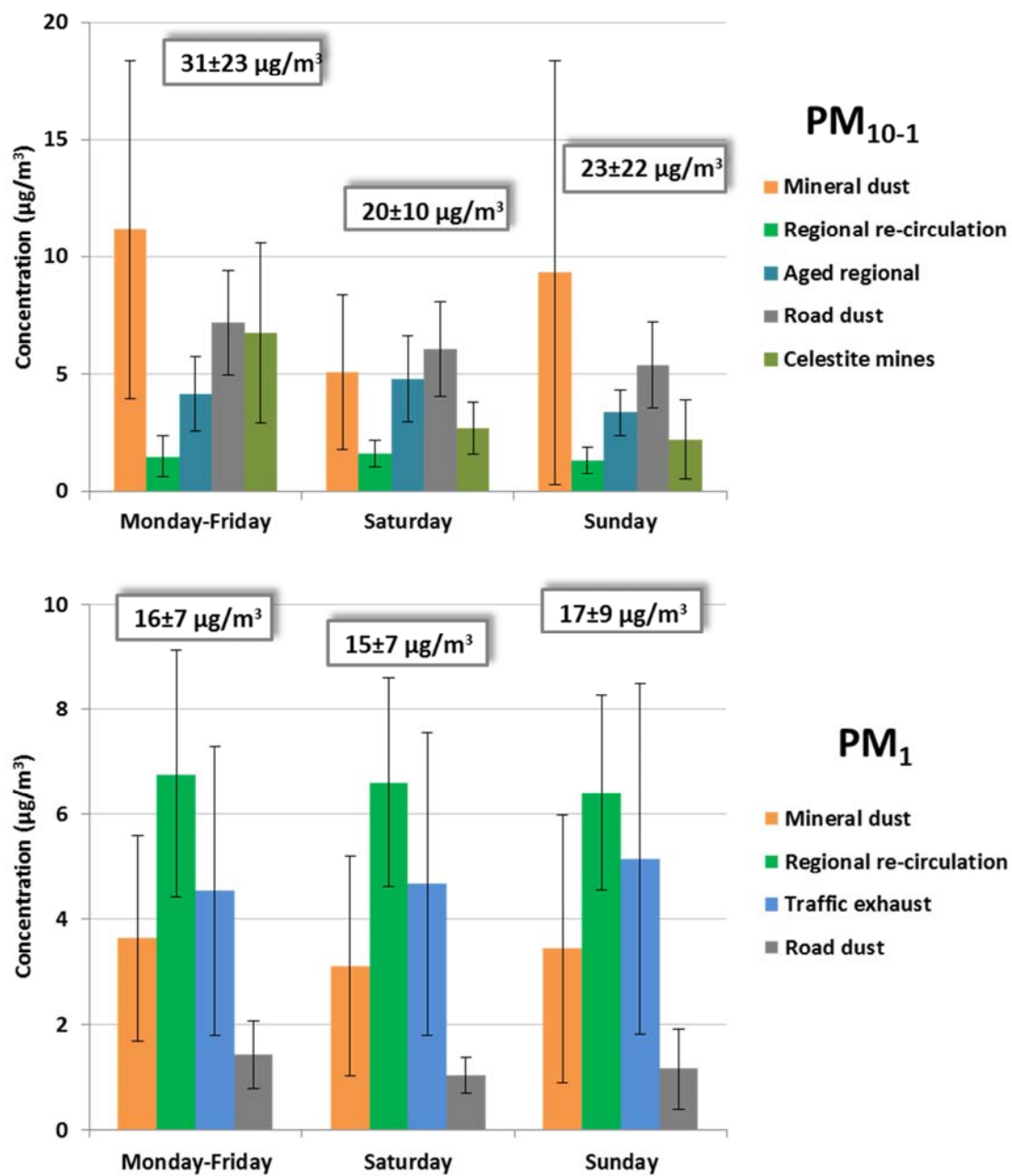
664

665

666

667   **Figure 1 (black and white)**
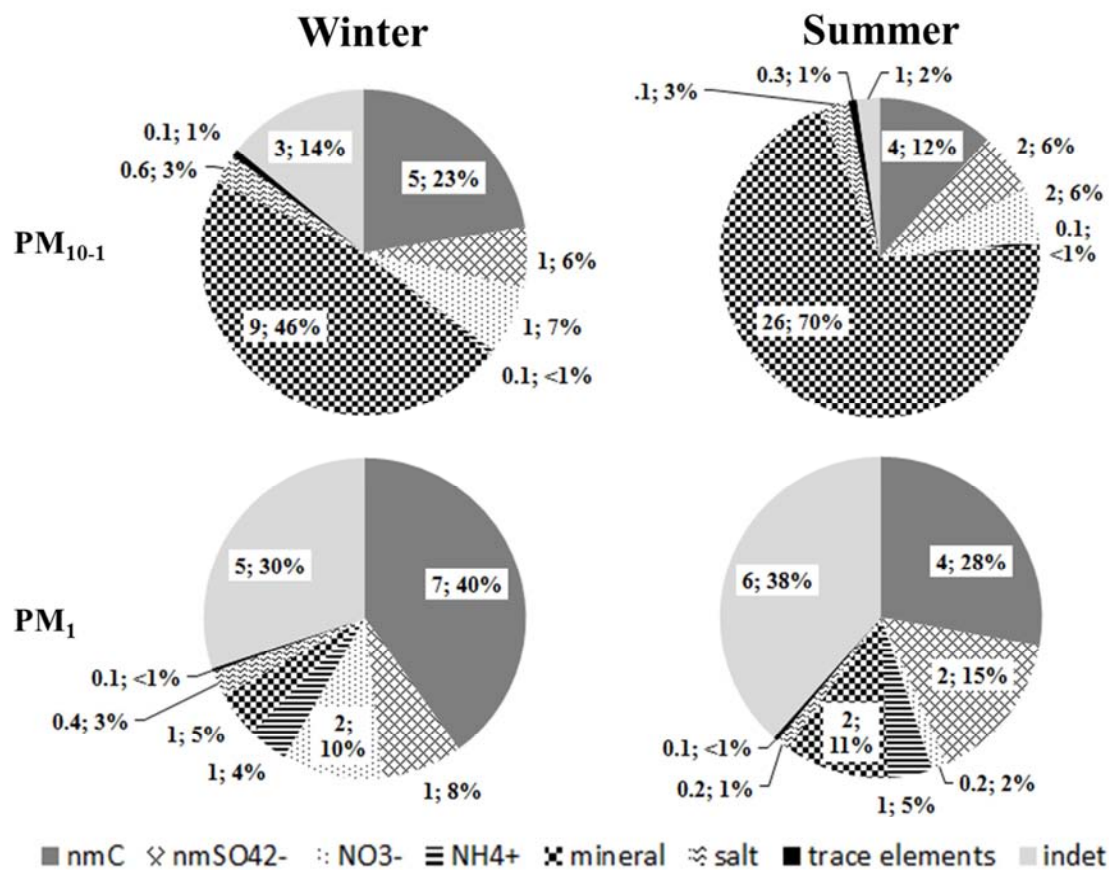
668

669

670

671

672

673

674

675   **Figure 2 (black and white)**
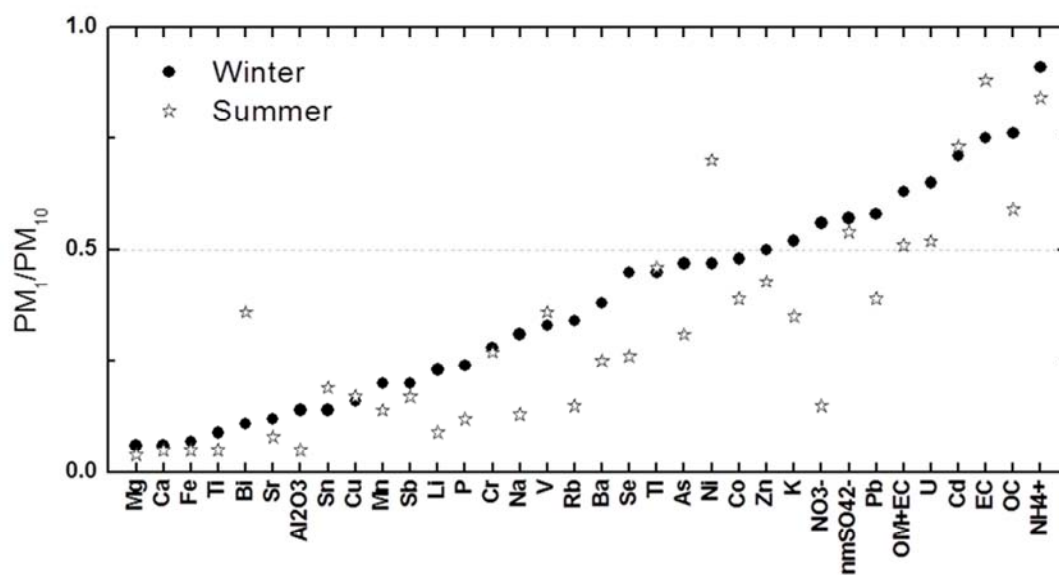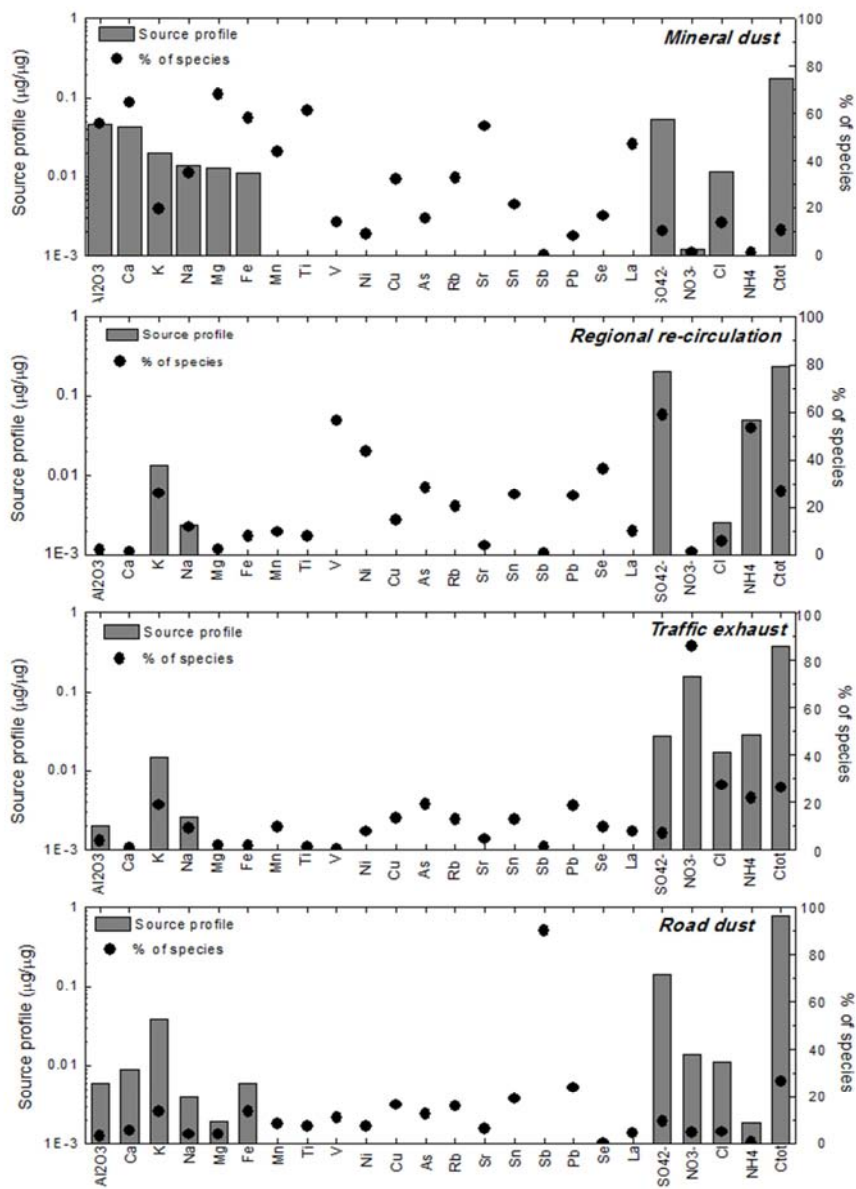

676

677

678

679

680

681

682

683

684

685

686   **Figure 3 (black and white)**
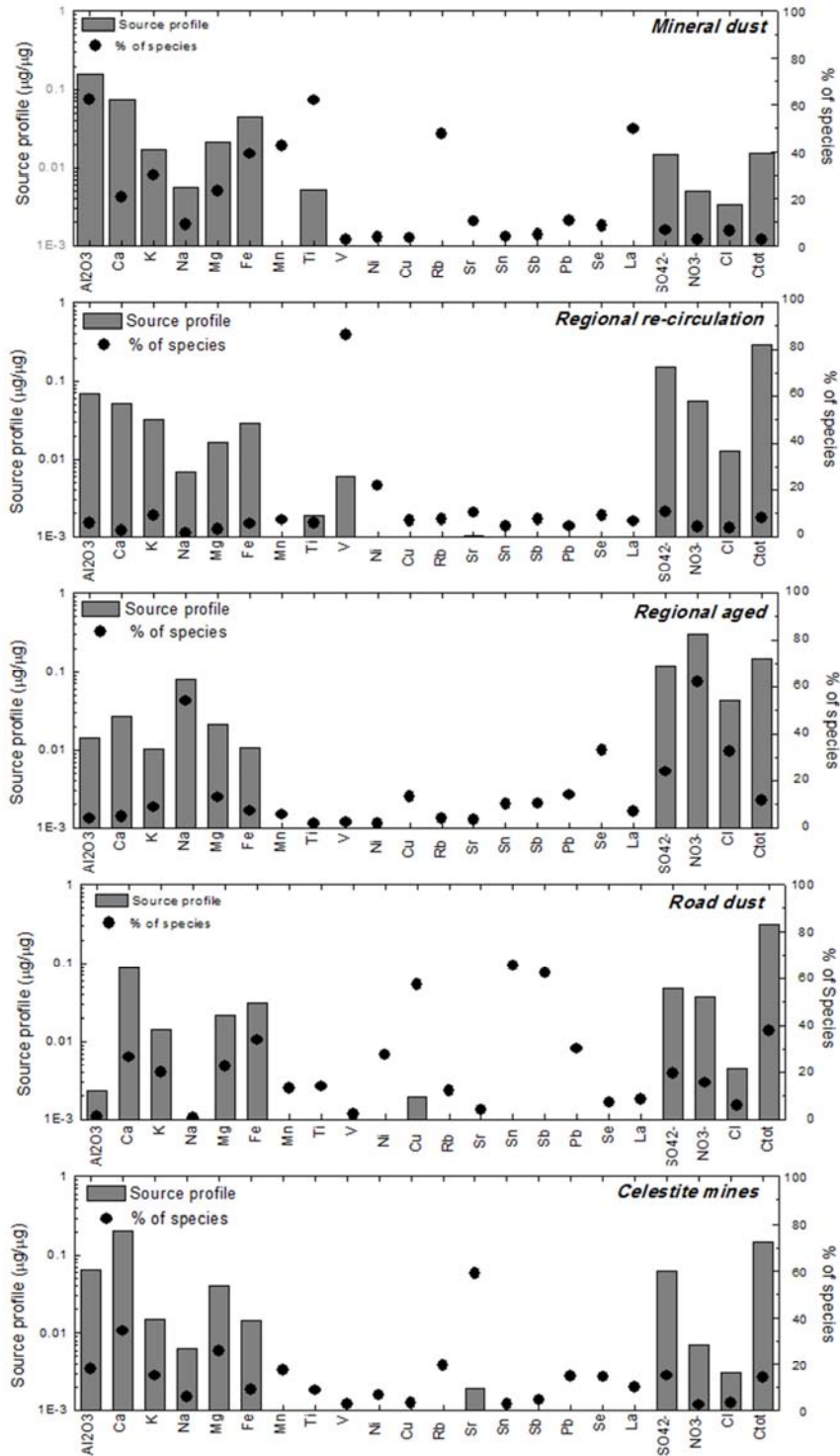
687

688

689   **Figure 4 (black and white)**

690

691

692

693

694 **Figure 5 (black and white)**
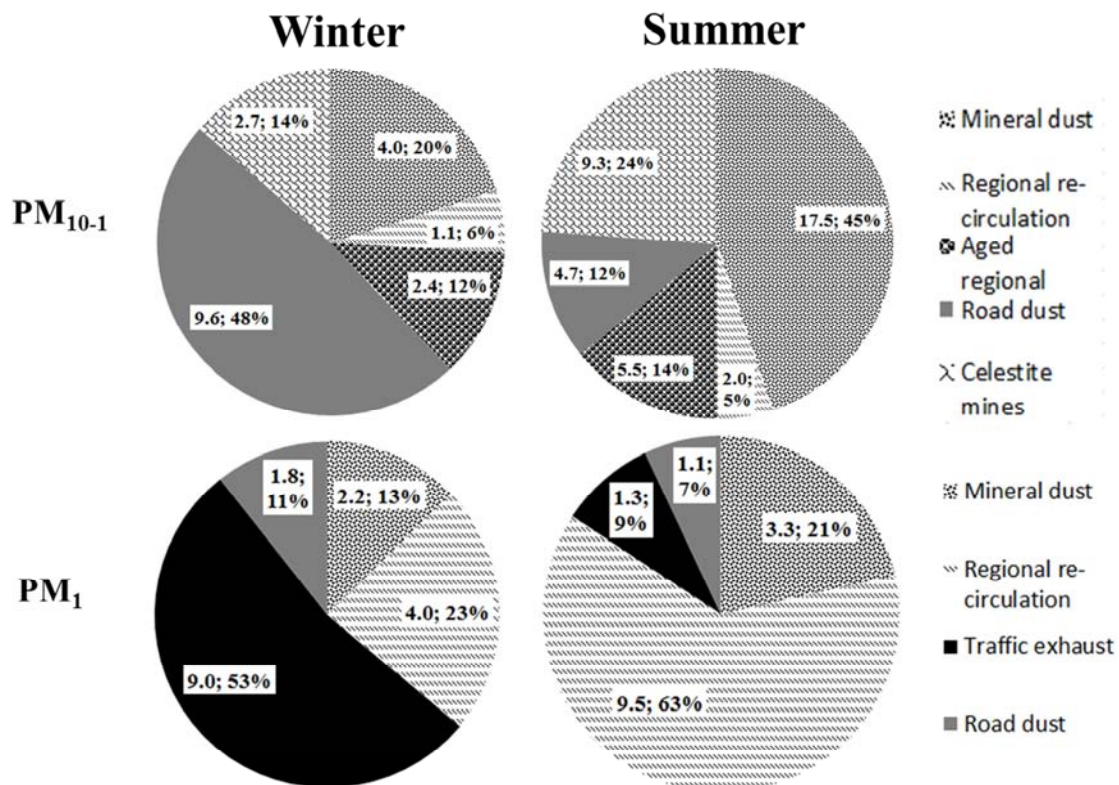
695

696

697

698

699

700

701

702

703   **Figure 6 (black and white)**

704

705

Winter

Summer

PM$_{10-1}$

- Mineral dust
- Regional re-circulation
- Aged regional
- Road dust
- Celestite mines

PM$_1$

- Mineral dust
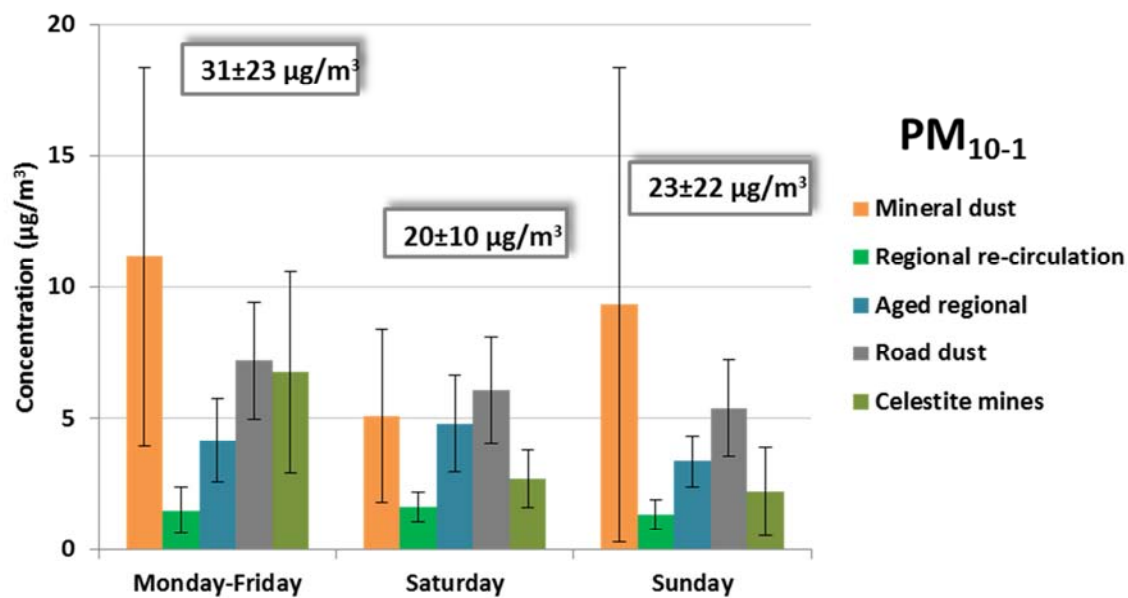- Regional re-circulation
- Traffic exhaust
- Road dust
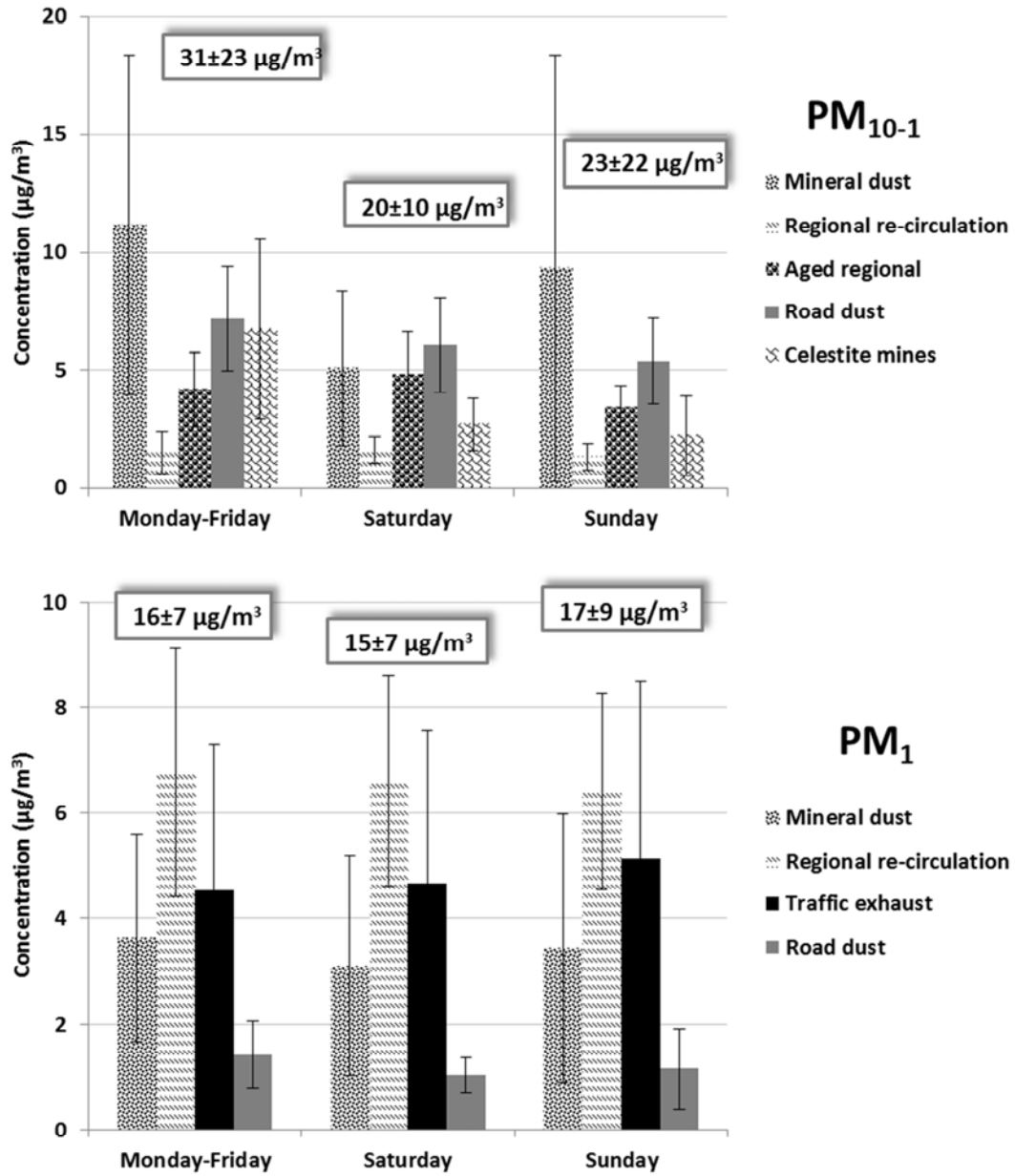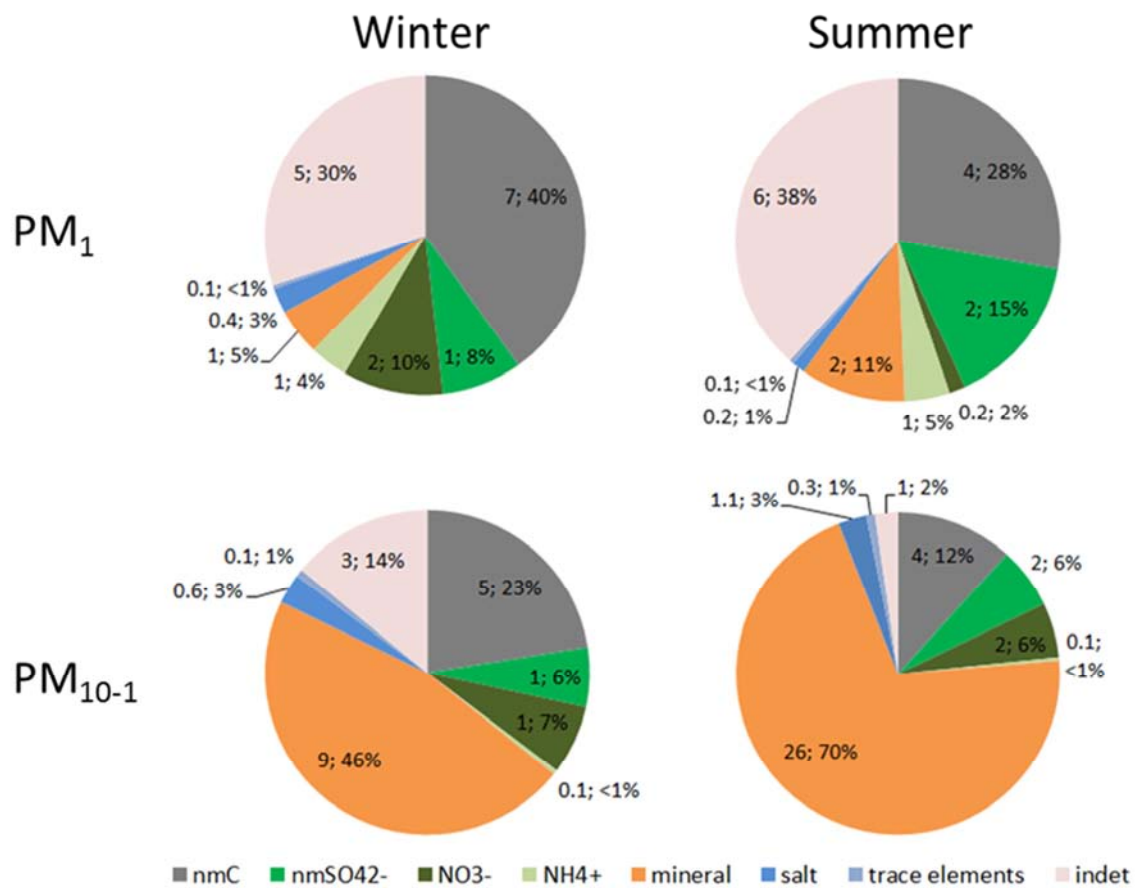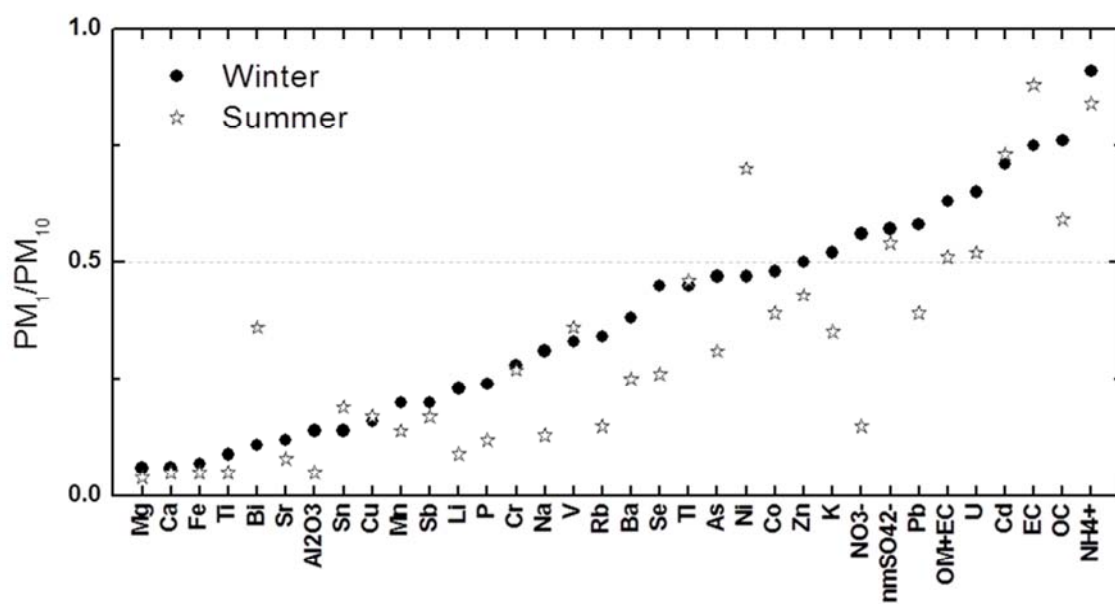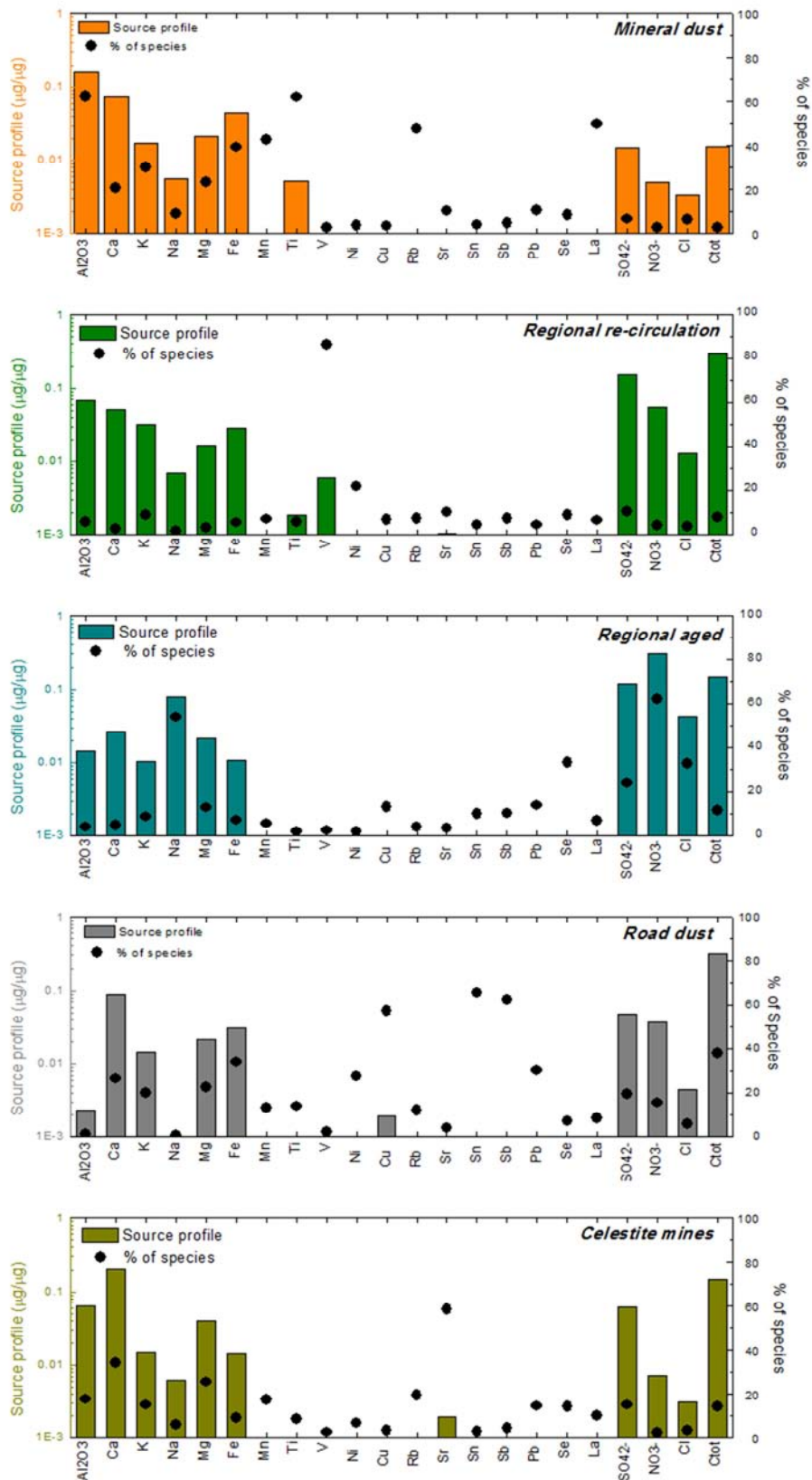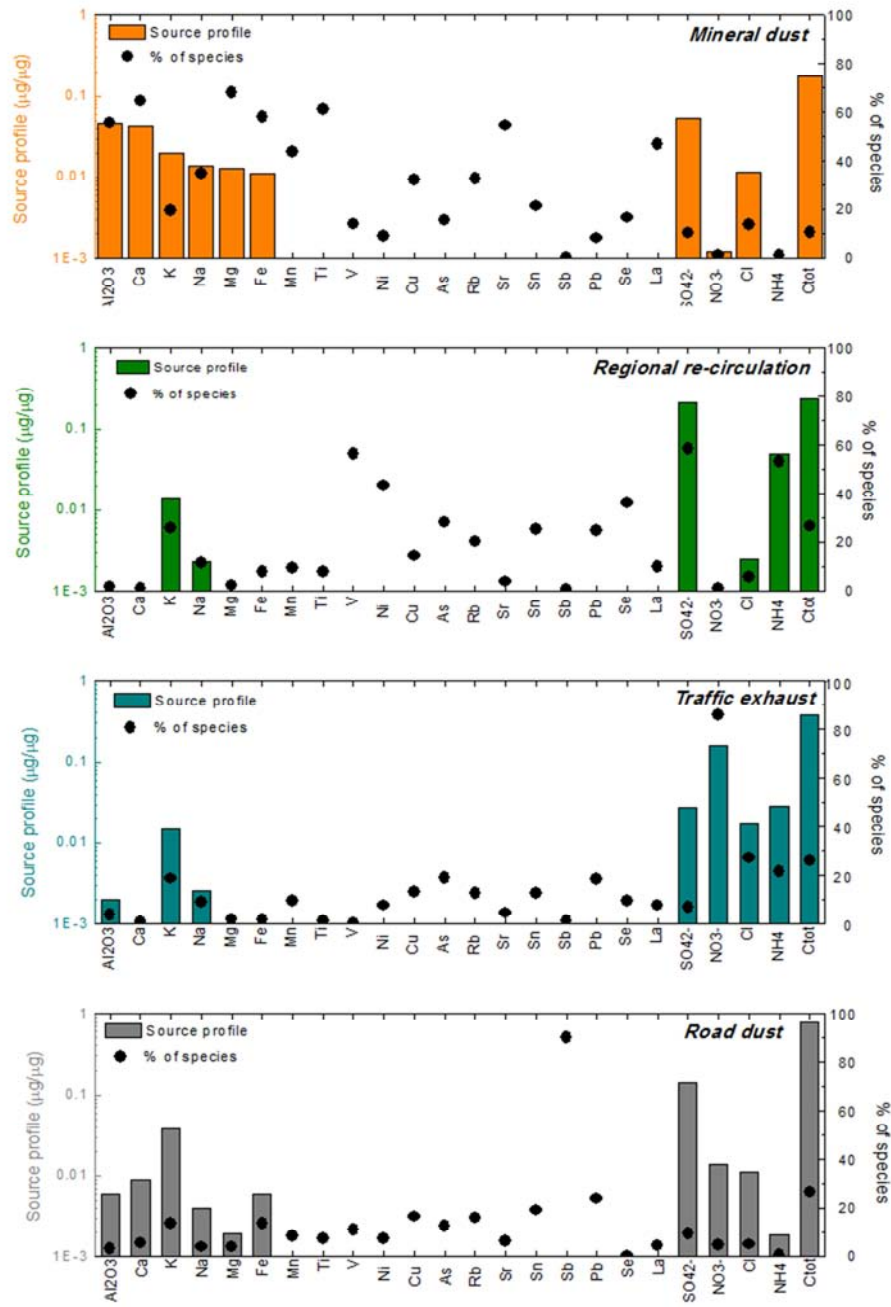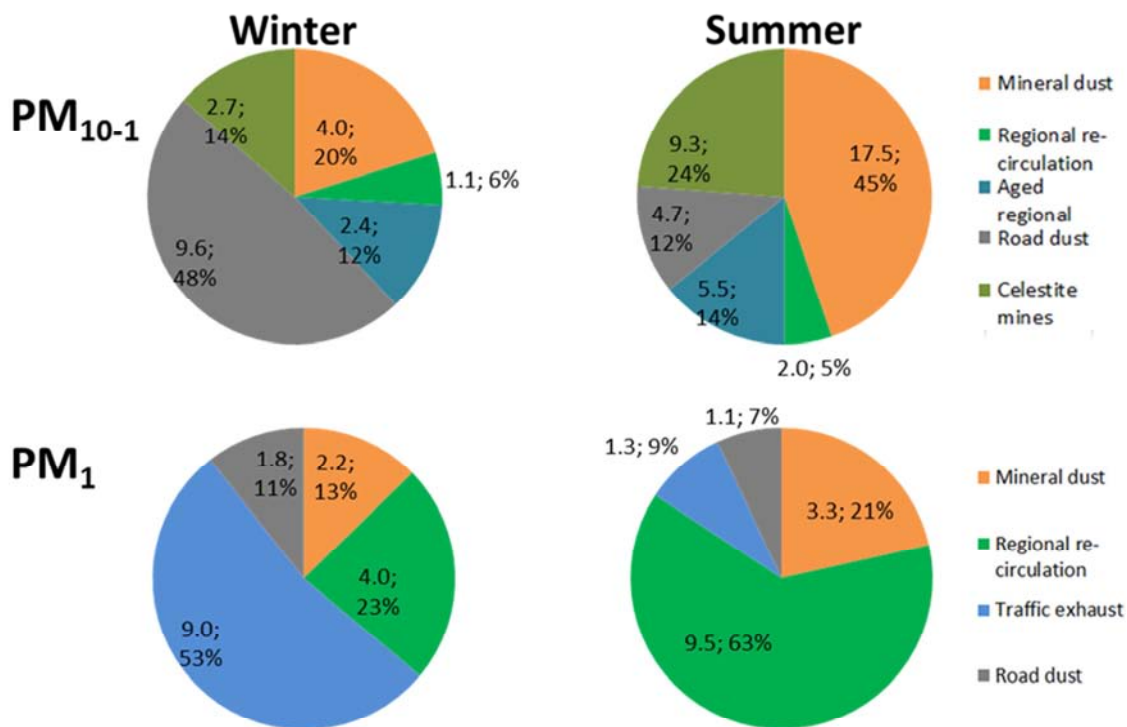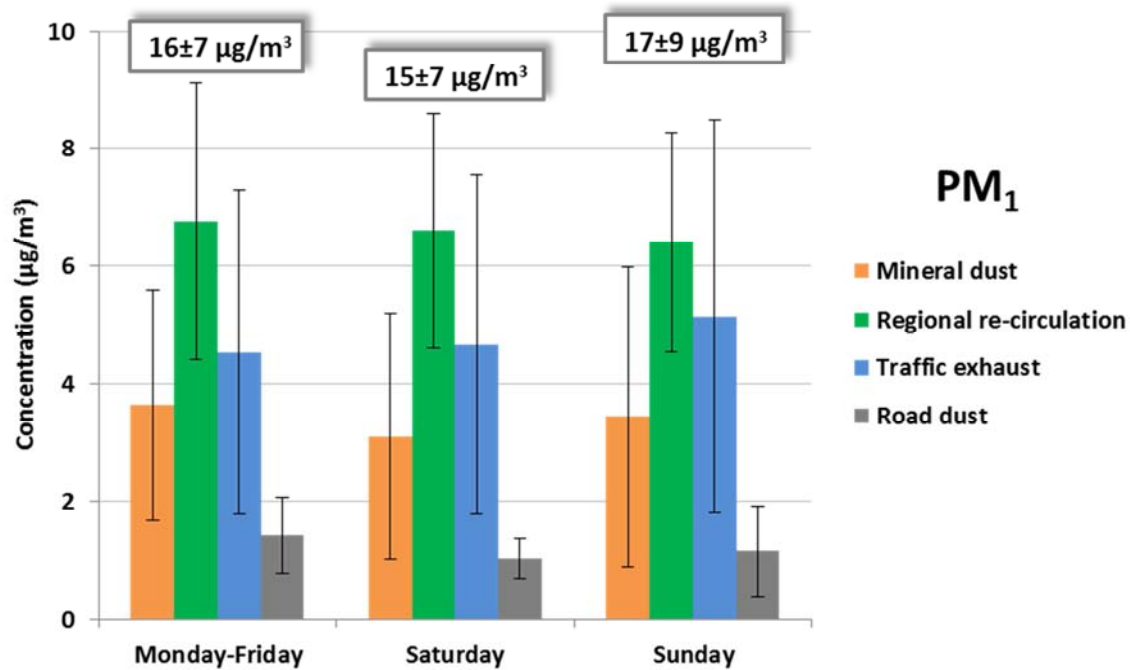
Highlights

1. Chemical composition of fine and coarse PM has been studied.
2. Decreasing trend was observed in the coarse fraction but not in the fine fraction.
3. PMF technique was used for the identification of fine and coarse sources.
4. To abate exceedances, traffic is the main source to target, especially in winter.

Suplementary material

Table S1: Mean, standard deviation (SD), percentage of data above detection limit (%ADL) and signal-to-noise (S/N) for the elements in the PM_{10-1} and PM_1 fractions included in the PMF analyses.

	PM_1				PM_{10-1}			
	Mean ($\mu g/m^3$)	SD ($\mu g/m^3$)	%ADL	uncensored S/N	Mean ($\mu g/m^3$)	SD ($\mu g/m^3$)	%ADL	uncensored S/N
Al_2O_3	0.2	0.5	37	3.8	2	3	100	8.1
Ca	0.2	0.2	46	2.4	3	2	98	8.4
K	0.3	0.2	57	3.4	0.5	0.4	73	5.4
Na	0.1	0.2	26	2.3	0.5	0.5	69	5.6
Mg	0.05	0.07	44	1.9	0.7	0.6	98	7.8
Fe	0.06	0.10	66	6.3	0.8	0.8	100	8.7
Mn	0.002	0.003	18	2.7	0.02	0.02	88	7.8
Ti	0.005	0.010	42	5.8	0.07	0.09	98	8.7
V	0.004	0.002	100	8.2	0.01	0.01	98	8.4
Ni	0.003	0.003	26	2.1	0.002	0.003	56	2.0
Cu	0.004	0.004	96	7.2	0.02	0.02	100	8.3
As	0.0003	0.0002	28	1.9				
Rb	0.0003	0.0003	39	2.7	0.002	0.002	88	7.6
Sr	0.001	0.002	18	2.2	0.02	0.03	93	8.1
Sn	0.0005	0.0002	26	1.6	0.003	0.001	98	7.0
Sb	0.0005	0.0006	90	8.1	0.003	0.002	100	8.4
Pb	0.004	0.003	100	7.7	0.005	0.006	98	8.1
Se	0.0002	0.0001	86	6.2	0.0003	0.0002	87	7.3
La	0.0001	0.0002	55	2.0	0.0006	0.0007	29	3.2
SO_4^{2-}	2	1	100	7.9	2	2	98	7.9
NO_3^-	1	1	99	7.9	2	1	99	7.9
Cl	0.1	0.3	42	2.1	0.3	0.5	45	2.0
NH_4^+	0.6	0.6	100	4.8				
Ct	5	3	99	2.4	4	3	89	5.3

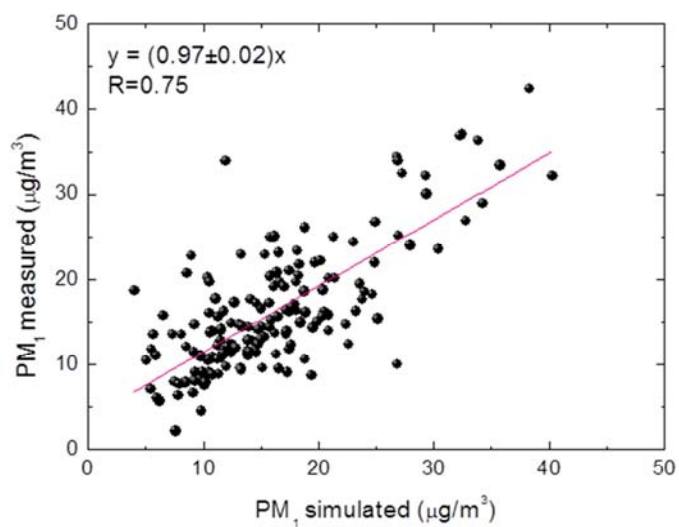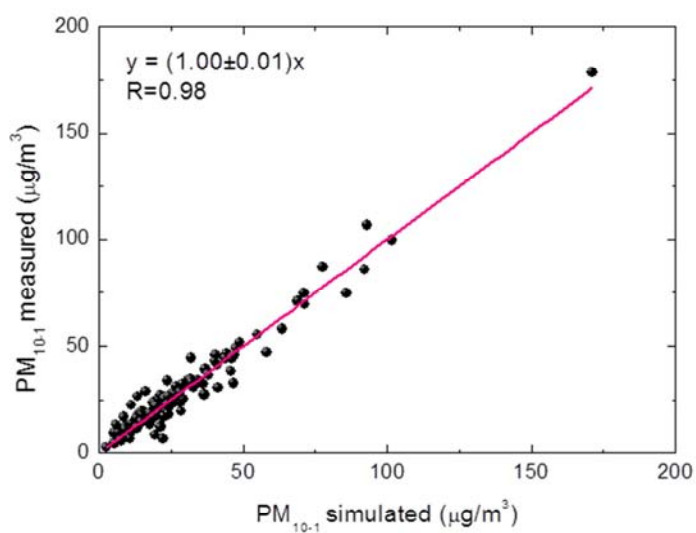**Figure S1:** Scatter plots of PM experimental versus PM simulated concentrations by PMF technique (in $\mu g/m^3$).

Figure S2: Contribution of sources to PM$_{10-1}$ (upper panel) and PM$_1$ (lower panel) expressed in μg/m^3 and corresponding percentage for the study period 2006-2010.
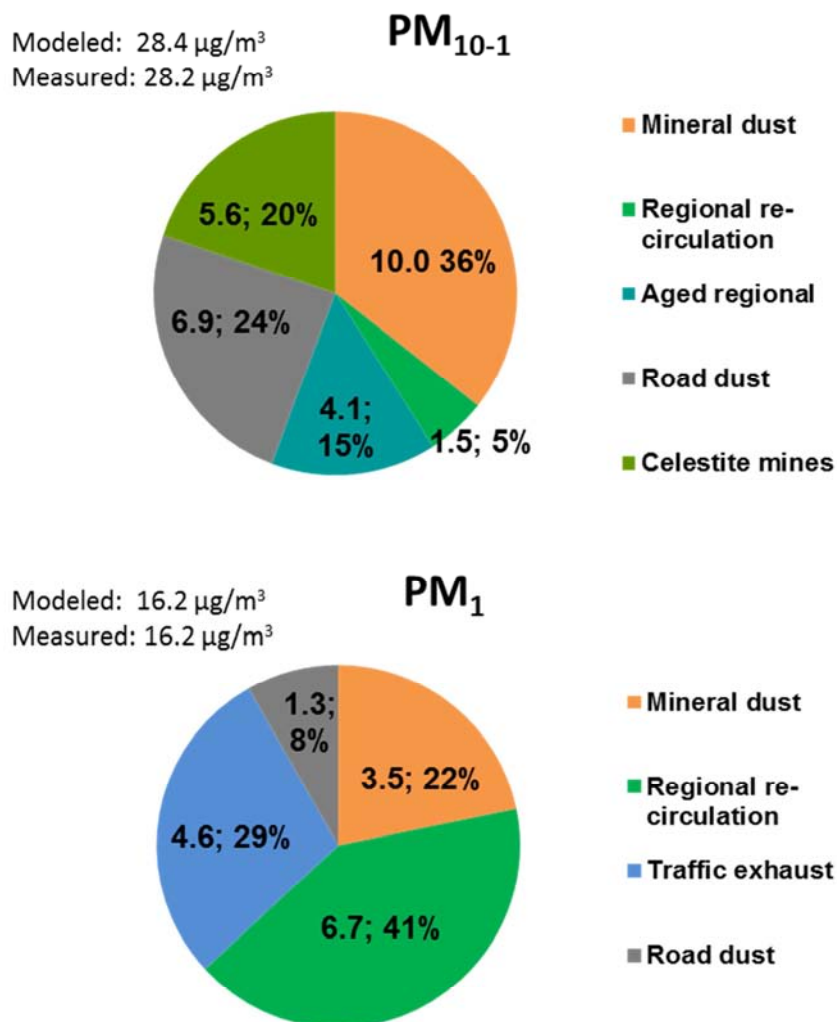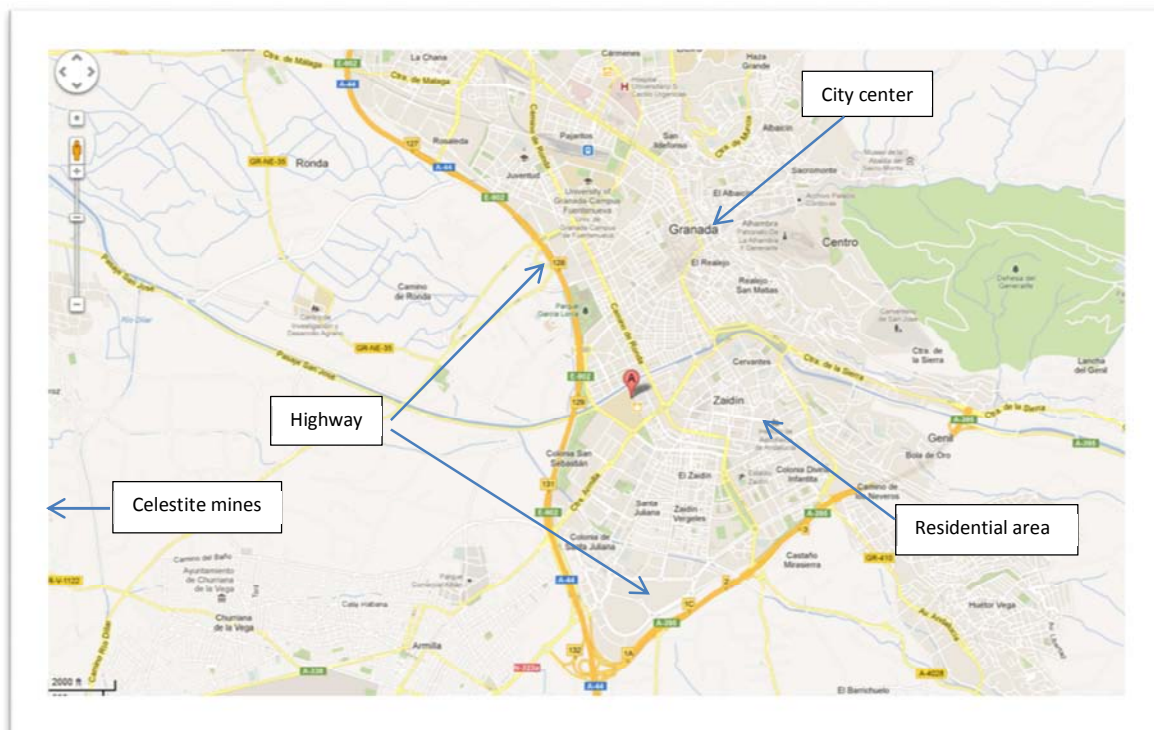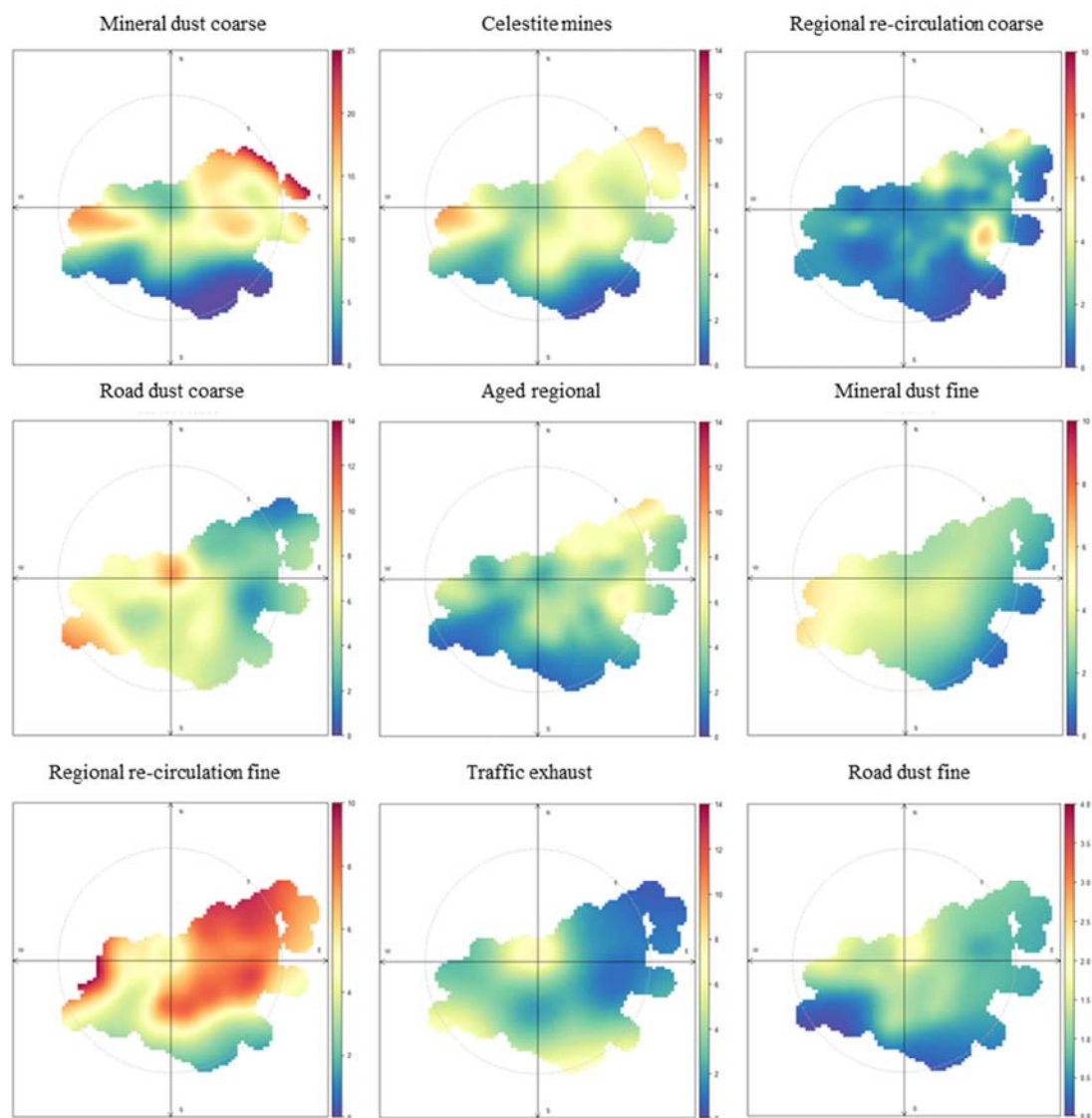
Figure S3: Location map (top) of the monitoring site and polar plots (bottom) of the PM source concentration in μg/m^3 obtained with PMF according to wind direction.

Mineral dust coarse

Celestite mines

Regional re-circulation coarse

Road dust coarse

Aged regional

Mineral dust fine

Regional re-circulation fine

Traffic exhaust

Road dust fine